Energy & Buildings 308 (2024) 114030

Contents lists available at ScienceDirect

Energy & Buildings

journal homepage: www.elsevier.com/locate/enb

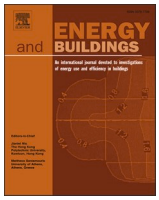

Enhancing climate resilience in buildings using Collective Intelligence: A pilot study on a Norwegian elderly care center

Mohammad Hosseini [a,*], Silvia Erba [b], Parisa Hajialigol [a], Mohammadreza Aghaei [a,c], Amin Moazami [a,d], Vahid M. Nik [e,f]

[a] Department of Ocean Operations and Civil Engineering, Faculty of Engineering, NTNU Norwegian University of Science and Technology, Ålesund, Norway
[b] Department of Architecture and Urban Studies, Politecnico di Milano, Milano 20133, Italy
[c] Department of Sustainable Systems Engineering (INATECH), University of Freiburg, 79110 Freiburg, Germany
[d] Department of Architectural Engineering, SINTEF Community, SINTEF AS, Oslo, Norway
[e] Division of Building Physics, Department of Building and Environmental Technology, Lund University, SE-223 63 Lund, Sweden
[f] CIRCLE - Centre for Innovation Research, Lund University, Box 118, 221 00 Lund, Sweden

ARTICLE INFO

Keywords:
Climate resilience
Aging population
Distributed decision-making
Energy flexibility
Vulnerable people
Reinforcement learning

ABSTRACT

The combined challenge of climate change and population aging requires novel solutions that enhance the resilience of building energy systems and secure indoor comfort for vulnerable occupants in extreme weather conditions. This research investigates the performance of a newly developed Energy Management (EM) system based on Collective Intelligence (CI) and Reinforcement Learning (RL), called CIRLEM, managing the energy performance of an urban complex in Ålesund, Norway, including an elderly care center with decentralized PV generation, EV charging and storage, while connected to a main electricity grid. CIRLEM controls multiple flexibility assets including independent thermal zones (the demand-side agents) and Electric Vehicle (EV) charging stations (the local storage). In a novel approach, CIRLEM coordinates the distributed storage and generation together with the demand side to control energy systems and react collaboratively to environmental variations. Under extreme weather conditions, without applying CIRLEM, the demand can be more than double that of typical weather conditions. The implementation of the double-layer CIRLEM can reduce the total demand by 35 % over a month. Furthermore, the inclusion of photovoltaic (PV) systems allows the system to be independent from the grid for almost 40 % of its operational hours, while adding EV storage can increase it to around 70 %. Finally, the application of CIRLEM reduced overheating hours from 17 h •°C to 2 h •°C under extreme conditions, while maintaining comfortable conditions even during temperature ramps.

1. Introduction

The confluence of climate change and rapid population aging has created a pressing need for immediate attention from researchers, policymakers, and planners. The pace of climate change has outstripped earlier predictions, heightening the likelihood of surpassing the 1.5 °C global warming threshold within the upcoming decade [1]. Moreover, the frequency and intensity of extreme weather events have been amplified by climate change [2]. Notably, the past twenty years have witnessed intermittent heatwaves associated with significant morbidity and mortality rates [3,4] culminating in July 2023 marking a historical zenith in temperature records [5]. According to the 2019 IPCC [6], Nordic countries have been met with the impacts of climate change at a rate higher than the global average, with the highest rate of country-specific warming [7]. At the same time, Europeans on average live longer than ever before, and the age profile of society is rapidly changing. It is projected that there will be close to half a million centenarians in the EU-27 by 2050 [8]. This will have profound implications on different aspects of society, such as urban development and housing, to meet the needs of the elderly and guarantee their well-being. The United Nations Sustainable Development Goals (UNSDG) 11 (sustainable cities and communities) identifies environmental impact reduction (Target 11.6) and resource efficiency and city resiliency (Target 11.b) as urgent international goals [9]. In parallel, SDG3 aims to ensure that people of all ages are guaranteed healthy lives and general well-being.

Extreme weather conditions such as heat waves and cold snaps, influence both the demand- and supply-side of building energy systems

* Corresponding author.
E-mail address: mohammad.hosseini@ntnu.no (M. Hosseini).

https://doi.org/10.1016/j.enbuild.2024.114030
Received 19 June 2023; Received in revised form 8 February 2024; Accepted 23 February 2024
Available online 24 February 2024

Nomenclature

Abbreviation

BEM	Building Energy Model
BIM	Building Information Model
CMIP5	Coupled Model Intercomparison Project 5
CI	Collective Intelligence
CIRLEM	Collective Intelligence + Reinforcement Learning Energy Management
CV(RMSE)	Coefficient of Variation ofthe Root Mean Square Error
DR	Demand Response
DSM	Demand-side Management
DT	Decision Tree
ECY	Extreme Cold Year
EMS	Energy Management System
EOL	End Of Life
EPW	Energy Plus Weather
EV	Electric Vehicle
EWY	Extreme Warm Year
FL	Federated Learning
GA	Grid Autonomy
HVAC	Heating, Ventilation, and Air Conditioning
IEA	International Energy Agency
LRM	Linear Regression Model
MDP	Markov Decision Process
NREL	National Renewable Energy Library
PMV	Predicted Mean Vote
PPD	Predicted Percentage of Dissatisfied
PV	Photovoltaic
RES	Renewable Energy Sources
RL	Reinforcement Learning
SAM	System Advisor Model
SCR	Self-Consumption Rate
SD	Standard Deviation
SOC	State Of Charge
TDY	Typical Downscaled Year
TS	Thermal Sensation
UN	United Nations
UNSDG	United Nations Sustainable Development Goals
WTL	Watch-Try-Learn

Variables

a	EV battery technical parameter [%]
E	Measured electric energy use
E_{EWY}	Total electricity use of the building in EWY
$\overline{E}_{TDY}$	Average seasonal electricity use in TDY
h	Hours of the analysis period
n(S)	Number of elements in the set S
n_d	Number of days in calculation
P	Probability of state-action combinations
$P_{load}^{(d,t)}$	Electricity load at t^{th} hour of the day d
$P_{PV}^{(d,t)}$	PV production at t^{th} hour of the day d
$P_{grid}^{(t)}$	Supplied electricity from the grid at time t
$P_{load}^{(t)}$	Building electricity load at timestep t
$P_{PV}^{(t)}$	PV production at timestep t
P_{max}^{EV}	Maximum instantaneous power for EV
SOC_i	Initial SOC of the EV in [%]
SOC_{max}	Maximum SOC for the EV [%]
SOC_t	SOC for each EV and time interval [%]
$SOC_{EV}^{(d,t)}$	SOC of EV at t^{th} hour of the day d

Parameters

t	timestamp
Δt	Time difference in each timestep
T	Measured outdoor air temperature
A	Action
R	Reward
S	State

[10]. On the demand-side, extreme weather may disturb a building's energy performance and the thermal comfort of occupants [11]. On the supply-side, unexpected and inordinate loads increase the risk of power outages and energy system disruption [12]. Impacts can become more pronounced when higher shares of Renewable Energy Sources (RESs) are integrated into the energy supply system, especially decentralized sources such as wind and solar power, due to their intermittent and climate-dependent nature [13]. RES penetration is expected to grow significantly by 2050 when distributed generation and storage are expected to have been widely implemented. Aggravated by the impacts of climate change, subsequent challenges will arise on the demand and supply sides, emphasizing the necessity of resilient energy systems [14]. A building's operation is highly dependent on its energy systems [15] which maintain indoor thermal comfort, run appliances, provide lighting, and other functions. Accordingly, being resilient is a vital characteristic of a viable and reliable energy system [16,17]. Meanwhile, a major concern about the climate resilience of energy systems is the increased energy demand during extreme weather events [18]. Although the design of building features can make its performance insensitive to typical climate and predictable extreme climate conditions, these features cannot be deemed protected in case of unforeseeable extreme events. In such instances, resilience is required, which focuses on withstanding and recovering during and after the occurrence of the event [19]. The United Nations (UN) defines the term resilience as "the ability of a system exposed to hazards to resist, absorb, accommodate, adapt to, transform and recover from the effects of a hazard in a timely and efficient manner" [20]. Therefore, being adaptable and flexible may increase the resilience of a system. The adoption of flexible strategies can improve the resilience of energy systems against extreme climate events [21]. This is even more crucial in the instance of elderly occupants as they are more vulnerable to critical overheating-related health issues such as exhaustion, dehydration, or even cardiac arrest which can occur during power outages [22].

Increases in mean life expectancy combined with evolving future climate scenarios and extreme events, underscore the necessity to investigate the dynamic and interactive relationship between the elderly and their living environments to guarantee their well-being and health [23,24]. Recent research by Wu et al. [24] found that elderly people experience a time lag and smaller variations in thermal responses than younger people when exposed to air temperature changes, particularly in non-neutral conditions. Younes et al. [25] developed a model for predicting the thermal experiences of the elderly under steady and transient states, helping to achieve thermally comfortable environments for elderly people with optimized costs. Jiao et al [26] studied the characteristics of the thermal environment in the transitional spaces of residential buildings occupied by the elderly and their impacts on the elderly's thermal adaptation. Several studies have shown that the differences between thermal perception and physiological response of the young and the elderly are relevant to distinguish between. Specific thermal comfort models for the elderly have been proposed in the literature [25,27,28]. In particular, Hughes et al. [22] proposed an age-corrected Predicted Mean Vote (PMV) model that could potentially produce relevant savings in energy use for winter heating. Hughes et al. argue that neither the PMV model nor the adaptive model accurately

predicted true thermal comfort during summer in naturally ventilated homes for the elderly [29]. Overall, researchers agree that further investigation is needed to predict the thermal comfort of elderly populations accurately [27].

Building energy systems are composed of various components such as weather parameters, human behavior, materials, energy market, etc. showing behaviors of a complex system [30]. Complexity in such a system arises because of the inter-relationship, inter-action, and interconnectivity of the entities within the system and between the system and its environment [31]. Entities in a complex system have agency characteristics, meaning individual agents' capability to decide and act independently [32]. In such an environment, the concept of resilience can be applied to the behavior of the participating systems, implying to show the attribute of flexibility as a vital element of a resilient system [33–35]. Flexibility and resilience are thus strictly related: energy-flexible buildings and communities can increase the resilience of the energy networks by reducing the stress on the infrastructure but also making the buildings and communities more resilient to fluctuations in the energy supply [36]. A recent study by Li et al. [37] emphasizes the contribution of building energy flexibility to energy system resilience pointing out the impacts of extreme events on peak loads magnitude and duration and disruption of RES generation. These conditions significantly affect the well-being of people, especially vulnerable populations where the capabilities of the building energy systems are prominent to maintain occupant comfort during adverse weather events.

The flexibility of the energy systems can be promoted both on the supply- and demand-side. The International Energy Agency (IEA) defines energy flexibility as "the ability for a building to manage its demand and generation according to local climate conditions, user needs, and grid requirements" [37,38]. Flexible operation of buildings is possible through Demand Response (DR) which is based on the power adjustment on the demand side in response to the grid requirements or price. DR programs may include flexibility programs, either automated or manual, voluntary or involuntary, and price-based or incentive-based. They are scalable at different levels, such as the level of the system/appliance, building, and district, with different features, including flexibility assets, timesteps, purposes, and flexibility signals (i.e., the trigger or the activator of the flexibility program) [39,40]. Timesteps can vary in length from seconds to hours based on grid requirements and flexibility assets whereas the last one refers to a specific energy component, strategy, or system that can be harnessed to modify energy demand or generation patterns to accommodate evolving circumstances [41,42]. Around 85 % of existing studies apply one or two different flexibility assets in their flexibility programs [39]. Flexibility on the demand-side can be generated through different strategies such as load shedding, load shifting, and load modulating [39,43]. The flexibility signal could be generated based on price, typical loads, RES production, or weather conditions [41].

Collective behavior within energy communities demonstrates improved performance in terms of control strategies aimed at enhancing resilience and flexibility [37] through the provision of multi-carrier energy systems and clusters of buildings. Continuously advancing smart and communication technologies are being employed in interactive flexibility programs [44] to facilitate energy flexibility on the demand-side in the cluster scale. In a previous work of the authors [35], the performance of Collective Intelligence (CI) to provide flexibility and resilience within clusters of buildings utilizing an advanced communication infrastructure is evaluated. CI is "a form of universally distributed intelligence, constantly enhanced, coordinated in real-time, and resulting in the effective mobilization of skills" [45] which is replicable within any large, distributed group of interactive agents with the least centralized control [46]. CI systems are complex by nature and can adapt their performance to uncertain and unknown conditions, organize themselves independently, and manifest emergent behavior [47]. Agents in a CI system perform Reinforcement Learning (RL) to improve their individual accomplishment and the performance of the whole system [48]. Interaction between agents improves their coordination within small groups of agents providing a cohesive behavior for the whole system while simple rules are applicable in smaller groups with less information about the environment and no central leadership [49]. Therefore, in such a structure of distributed intelligence, decision-making can happen at the agent level (distributed decision-making) which distributes computational power [50] while reducing data sharing leading to higher privacy and security [51].

Reinforcement Learning shows adequate performance in energy systems control [52,53]. Krishna G.S. et al. [54] suggest a diversity-induced RL algorithm to improve training processes without sacrificing thermal comfort. Qui et al. [55] model a building community as a multi-agent RL to provide flexibility to building energy management while using Federated Learning (FL) to accelerate training and enhance privacy. Shen et al. [56] aim to reduce the energy cost of HVAC systems by increasing the utilization of RES by applying a multi-agent, cooperative control strategy based on deep RL to achieve an optimal match between the supply- and demand-side. Khan et al. [57] study a cluster of smart homes with smart appliances to quantify the performance of RL to reduce energy use and discomfort, applying transfer learning to enhance the learning process when there is minimal or no training data. Syed Asad et al. [58] propose distributed control and computation with independent decision-making in an HVAC system to improve energy efficiency. Zhang et al. [59] employ a model-free deep RL to evaluate the effectiveness of EVs in adjusting supply and demand to minimize operating costs and satisfy charging expectations. The integration of RL into CI-based energy management is investigated by Nik & Hosseini [60].

Demand-Side Management (DSM) encompasses various methods that can modify energy consumption patterns and levels by reducing, increasing, or rescheduling energy demand. Since the early 1980 s, DSM has been recognized as a valuable tool for shaping energy demand [61]. It contributes to the growth of distributed energy generation, facilitates the decarbonization of energy systems, improves the reliability and security of energy supply, and delays the necessity for new network infrastructure investments [62]. RESs can experience fluctuations in supply due to changes in climate conditions. DR represents a dependable and efficient approach to seamlessly incorporate renewable energy sources by leveraging load flexibility as needed by the system [63]. Considering the inclusion of multiple parameters in DSM-based solutions such as various sources of energy, weather conditions, volatile RES generation, and different user needs and preferences, increases the complexity of the energy system management compared to traditional approaches and makes them less competitive [62]. In addition to adopting technology-focused methods, it's essential to cultivate occupant-centric approaches and information-based methods, offering comprehensive solutions [64]. Simpler techniques that have the potential to enhance user participation are required [65] incorporating human feedback into the control process to mitigate user discomfort [66]. Additionally, there is a requirement to advance methodologies for quantifying costs and benefits, establishing market structures, and creating incentives [62]. In this context, data-driven solutions, such as machine learning [67] or reinforcement learning [66], can prove beneficial. Nevertheless, addressing the challenge of managing big data and user privacy remains an ongoing concern. This work aims to address the current issues in applying DSM to make them more practical and attractive by proposing a DSM and Energy Management (EM) algorithm with a focus on user comfort, operating with less amount of data storage while no private data sharing is required.

In Norway, the population of more than 70 years old people is projected to grow by 200 % to 1.4 million in 2050 [68] while the country encounters severe heatwaves as a consequence of climate change [69,70]; thus, climate resilient elderly accommodation become prominent. The previous work of the authors [71] addresses the performance of a DSM using a light-weight algorithm to increase the resilience of an elderly care center in Norway facing extreme warm weather. An energy management approach is further developed by

combining RL into CI showing outstanding performance on EM under extreme weather conditions called "CIRLEM" (CI + RL + EM) [60]. CIRLEM presents a notable enhancement in energy flexibility and climate resilience for a cluster of buildings, guaranteeing energy conservation while maintaining indoor comfort at the standard level.

The transition from centralized to decentralized energy systems showing enhanced flexibility and efficiency [72,73], brings new perspectives in climate resilient buildings by the inclusion of distributed generation and storage. However, additional energy systems (i.e., distributed generation and storage) rise the complexity and cause the curse of dimensionality, which requires developing solutions to deal with a large number of control variables [13,74]. This research deploys a CIRLEM algorithm which, in a novel structure, exploits a double-layer learning algorithm, namely (1) *meta*-learning and (2) try-watch-learn, to accelerate the training process. To challenge CIRLEM, in addition to the demand side in the energy systems, distributed generation and storage are included in the system, leading to a higher degree of complexity and computation. This research aims to explore and evaluate the capabilities and performance of the proposed CIRLEM structure by deploying a high-resolution Building Energy Model (BEM) to achieve an accurate assessment of energy performance and thermal comfort. In addition to the creation of the *meta*-learning phase, compared to the previous work of the authors [60], this work contributes to further developments by adding the following components to CIRLEM to assess the performance with more complexity induced by additional energy systems:

a) Electric Vehicles (EVs) as storage facilities (distributed storage).
b) Photo Voltaic (PV) system as the local generation (distributed generation).
c) Four adaptation measures namely, temperature setpoint, ventilation rate, equipment load, and EV storage.

The evaluation is carried out on a pilot case in Norway, which is fully equipped with an Energy Management System (EMS), Photovoltaic (PV) station, Electric Vehicle (EV) chargers, and ventilation systems. The methodology in chapter 2, introduces the algorithm, data collection, and modeling process. Chapter 3 presents the results and analysis followed by the conclusion.

2. Methodology

This research investigates the performance of a CIRLEM algorithm, designed to increase the resilience of building energy systems [60]. Cooling systems are not common in Scandinavian buildings due to historically cold summers [75]; however, the increasing frequency of heat waves has introduced the risk of thermal discomfort [76,77]. A building in Norway that accommodates elderly people was selected for the pilot case study building, to provide the most restrictive thermal comfort conditions. Weather data representing a warm summer were used from the analysis period of July 2050. The analysis is carried out on a 15-minute timescale to achieve a realistic understanding of extreme conditions and HVAC system performance. A high temporal resolution dataset, including energy and indoor temperature, is produced by the pilot case with an hourly timescale. Various energy systems are installed in the building including a PV station, an EV charging station, EMS, and a Heating, Ventilation, and Air Conditioning (HVAC) system. In this research, "measured electric energy use" refers to the measured delivered electrical energy for all purposes from the grid to the building, and "simulated electric energy use" refers to the summation of electric energy uses for cooling, heating, ventilation, lighting, and equipment (plug load) obtained via energy simulation. This chapter describes the pilot case, weather datasets used for the purpose of this research, the Building Energy Model (BEM) and calibration process, the CIRLEM algorithm, and its components, and finally evaluation indicators.

2.1. The pilot case

The pilot building is an elderly care center in Ålesund, Norway, consisting of five stories, 70 residential units, 40 public rooms and offices, and a total floor area of 7000 m^2. The building is equipped with EMS, which controls and monitors heating and cooling systems, ventilation, domestic hot water, and lighting. The EMS can send commands to each controller in the building to change their condition and capture the metered values for electricity, warm water, and conditioned air (i.e. flow and temperatures). The pilot building was built in 2017 with high-performing building components and systems. According to Norwegian law, building owners are obliged to obtain energy certificates through periodic assessments. Therefore, an adequate database of building specifications and the Building Information Model (BIM) is available for the pilot building. The envelope characteristics are described in Table 1 and a photo of the building is presented in Fig. 1.

There is a 170-kWp roof-top PV station with around 1000 m^2 panel surface area which produces approximately 100 MWh over a year. There are five low-voltage EV charging points that are supplied by the delivered electric energy to the building. The primary sources of energy are electricity from the grid and PV production, which account for 82 % and 18 % of annual electricity use, respectively. During the analysis period in this research (July 2050), the share of PV production increases to around 34 % and the grid electricity usage decreases to 66 %. The measured electric energy use and PV production (annually and in July) are presented in Table 2, where the share of the electricity source is denoted. Fig. 2 illustrates the distributions of delivered electricity and PV production in July in three years with a maximum hourly production of around 120 kWh and average production around 25 kWh.

2.2. Weather data

Two sets of weather data are used in this research. The first one is the historical data which is used for BEM calibration. The measured data is on an hourly scale, including the major parameters necessary for an energy simulation (air temperature, relative humidity, direct and diffuse solar radiation, wind speed and direction, and cloud index). Measured data is adapted to an Energy Plus Weather (EPW) file. The data corresponds to the period of 2019–2021. The second set of weather data is future weather data and is used to evaluate the algorithm's performance under future climate conditions. The future weather data is generated using 13 future climate scenarios from the "Coupled Model Intercomparison Project 5″ (CMIP5) over the 30-year period of 2040–2069, which we consider as the representative period of the 2050 s. Two sets of future weather data are generated based on the method developed by Nik [78], namely the Typical Downscaled Year (TDY) and Extreme Warm Year (EWY), representing typical and extreme warm conditions, respectively. More details about creating future climate weather data sets suitable for energy simulations are available in [79]. Fig. 3 shows the distribution of outdoor air temperature in July for historic and future weather data. The monthly average temperature under EWY-2050 is 17.7 °C, and under TDY-2050 is 13.9 °C, which demonstrates the difference between the typical and extreme conditions. Moreover, the differences in mean and minimum temperature values between historic values and future data, are significant. The boxplot of historical weather data shows that below-zero temperatures in July and the 1st quartile (25 % of the hours) were lower than 8 °C. The considerable differences between the current and

Table 1
Building envelope thermal transmittance (U-value).

Building component	U-value [W/m^2K]
Vertical opaque walls	0.12
Windows (Glazing and frames)	0.85
Slab on the ground	0.15
Roof	0.13

Fig. 1. The pilot building consists of 5 stories, the southern façade.

Table 2
Measured electric energy use and PV production over three years for annual and monthly periods. The ratio of delivered electric energy and PV production is mentioned in percentage.

		Measured electric energy use [MWh]	Measured PV production [MWh]
Annual	2019	623 (85 %)	104 (15 %)
	2020	657 (86 %)	106 (14 %)
	2021	727 (92 %)	61 (8 %)
July	2019	36 (62 %)	22 (38 %)
	2020	41 (68 %)	19 (32 %)
	2021	43 (66 %)	22 (34 %)

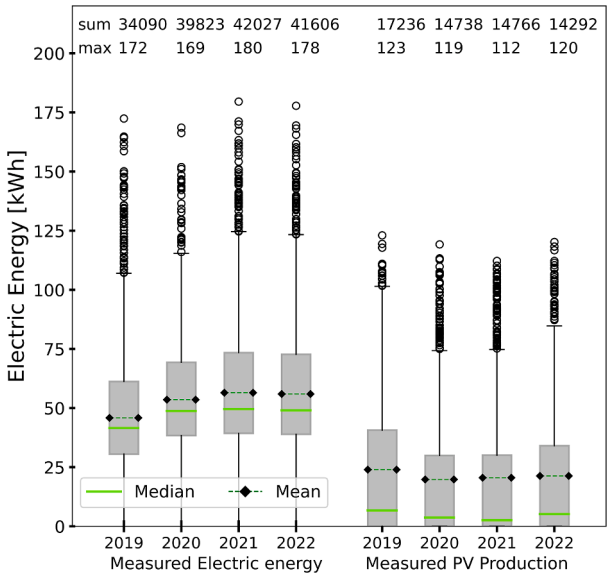

Fig. 2. Measured delivered electricity and PV production in July from 2019 to 2021. The major statistical values for each boxplot are denoted on the top, including the total value (sum), mean value, and maximum.

future conditions emphasize the risk of thermal discomfort and energy system malfunction under future climate conditions.

2.3. Building energy model (BEM)

A high spatiotemporal resolution Building Energy Model (BEM) is deployed to simulate the deployment of the algorithm's control of the

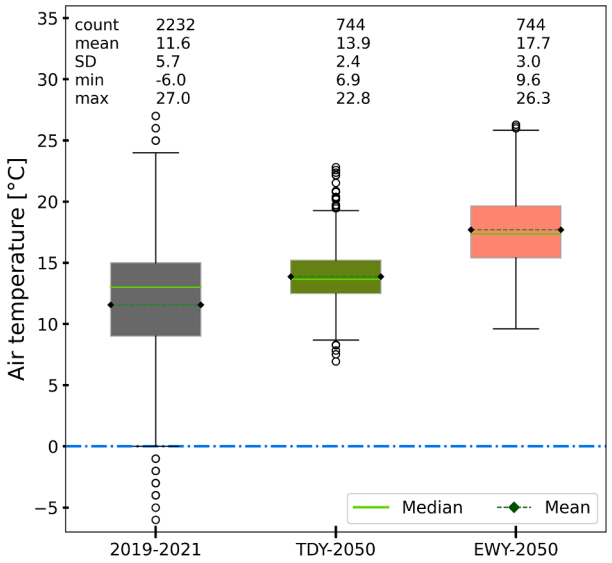

Fig. 3. Outdoor air temperature distribution in July for historic and future weather. The major statistical values for each boxplot are denoted on the top, including the number of values (count), mean value, standard deviation (SD), minimum, and maximum.

EMS [76]. The BEM is developed in the dynamic building energy simulation program Energy Plus [80]. A High-resolution geometry is developed in the 3D modeling software Rhino which allows the geometry to be coupled with Energy Plus using the Ladybug/Honeybee tool [81]. This produces accurate geometry (including balconies, shadings, rooms, etc.) based on the IFC files provided, where IFC files contain BIM data [82]. Open Studio is used to add the HVAC system to the energy model. Open Studio enables the addition of the HVAC system in detail. Energy Plus version 8.9.0 and Open Studio version 2.5 are used for building energy modeling.

To achieve a reliable model, the BEM must be validated. Thus, the BEM is calibrated against measured electric energy use on an hourly scale over a year (8760 h), according to ASHRAE Guideline 14–2014 [83]. The calibration is a part of the Measurement and Verification process which utilizes the Coefficient of Variation of the Root Mean Square Error (CV(RMSE)), and Normalized Mean Biased Error (NMBE) based on Eq. (1) and Eq. (2). $\hat{y}$ stands for simulated data, y is measured data, $\bar{y}$ is the average of the measured data, and n represents the total number of values. p is recommended to be equal to 1 [84]. Within the calibration, BEM should include thermal mass effects, 8760 h per year,

operation and occupancy schedules, and actual weather data. Using hourly timesteps, the BEM is considered calibrated if |NMBE|<10 % and CV(RMSE) < 30 %.

$$CV(RMSE) = \frac{1}{\bar{y}}\sqrt{\frac{\sum_{i=1}^{n}(y_i - \hat{y}_i)^2}{n-p}} \quad (1)$$

$$NMBE = \frac{1}{\bar{y}}\frac{\sum_{i=1}^{n}(y_i - \hat{y}_i)}{n-p} \quad (2)$$

Aiming at minimizing the values of CV(RMSE) and NMBE, the BEM is modified by iterating in a set of values building characteristics and internal gains which are mentioned in Table 3. The iteration and modification of BEM is done by a Grasshopper script including Galapagos component. Galapagos is a native Grasshopper component which, instead of trying all the possible combinations of the parameters, utilizes genetic algorithm to converge to the defined target (i.e., minimizing CV (RMSE) and NMBE) having common applications for architects and building designers [85].

Given the importance of indoor thermal comfort in this research, the second calibration is performed on the inherited model from the prior calibration process as it showed proper performance in similar cases [86]. In this process, the model is calibrated against measured indoor air temperature over June, July, and August 2022 for four sample rooms. This is to achieve a more accurate building model and internal thermal mass and to achieve a better estimation of indoor thermal comfort in the simulation given that thermal comfort assessment is a focal area of this research. The calibration process is carried out by tuning the mentioned parameters in Table 3 in a ± 10 % range iteration. In addition to the BEM, extra energy systems must be imported into the model, including the PV station and EV charging points. The PV station model is developed and calibrated using System Advisor Model (SAM) [87], open-source software developed by the National Renewable Energy Library (NREL) [88]. SAM provides a parametric study tool that is beneficial for the calibration process. The model is calibrated against the measured electricity production of the PV station over the 2019–2021 period.

2.4. Modeling of electric Vehicles (EVs)

Modeling and importing EVs into the algorithm as on-site storage is vital due to the lack of other storage within the system. However, the primary purpose of the EVs is to meet the travel needs of users, EVs are also considered as electric energy storage which serves the building energy systems as local storage. Local storage can be beneficial for peak shaving and load modulating. A stochastic approach can be deployed to address the uncertain presence of EVs, their State Of Charge (SOC), and load demand [89]. Zhang et al. [59] apply a stochastic distribution to generate random behavior of EVs, which is used in this research to simulate the EV charging process, the arrival SOC, presence, and capacity. The presence of EVs is defined according to the measured electricity of EV chargers over three years. The hourly data for July 2019, 2020, and 2021 is compiled and organized on a weekly basis keeping the weekdays and hours of the day fixed. This means that for each hour on a Monday, for example, there are measured values spanning three years and four weeks, providing a comprehensive overview of the variations and trends during that specific hour across multiple years and weeks. Afterward, a random value is generated based on the probability of the occurrences of the values under each hour of each day of the week (e.g., 14:00 on Wednesday including all the values for 14:00 on all Wednesdays in July 2019–2021) for the entire analysis period. This can represent the EV charging schedule based on the actual conditions in different days and hours considering the real EV users (employees and visitors) on the certain day of the week and the hour of the day. Fig. 4 illustrates the stochastic distribution of EV presence at charging points based on the number of hours over the analysis period (31 days). The heatmap shows the presence of an EV at each charging point from 0 to 12 h in a day.

Table 3
BEM Calibration parameters intervals and steps.

Parameter	Interval	Step
Extrerior walls U-Value [W/m^2·K]	0.08 – 0.16	0.01
Roof U-Value [W/m^2·K]	0.08 – 0.16	0.01
Slab on the groud U-Value [W/m^2·K]	0.08 – 0.16	0.01
Windows U-Value [W/m^2·K]	0.8 – 1.2	0.05
Windows g-Value [%]	40 – 60	5
Infiltration rate [h^{-1}]	0.5 – 0.8	0.05

The EV battery life depends on the charging-discharging cycles. The influence of the self-discharge rate is ignored. Fig. 5 is a piecewise function that represents the manufacturer's recommendations for the discharging process of EV batteries [90]. The figure shows there are two technical limits for charging and discharging the batteries, namely, the minimum and maximum SOC (SOC_i and SOC_{max}) levels at maximum power (P_{max}^{EV}). Moreover, between the SOC_i and a (an EV battery technical parameter), the discharge power is limited by a linear function which is dependent on the punctual SOC (SOC_t).

Unsuitable charging approaches will result in dramatic economic loss caused by rapid battery capacity degradation, which cannot be overlooked because the price of EV batteries is nearly half of the vehicle price [91]. To prevent a low partial load efficiency of power electronics, it is assumed that the minimum charging power is 10 % of the charging power rating [92]. It is also assumed that EVs can discharge only twice a day, and they will leave the station with at least 10 % more SOC than the SOC on arrival, as a guarantee that they will have enough charge to reach another charging station. The capacity of each EV battery is set to 40 kWh as the average value of typical EVs. EVs can also only be charged from PV generation and do not use grid electricity. More EV characteristics and EV charging points specifications are denoted in Table 4.

2.5. CIRLEM algorithm

Enabling flexibility in an environment could activate or improve the resilience of that environment [34]. Additionally, the collective behavior of entities within a complex system enables them to act as a unified whole making the cohesion in the system as a vital attribute of a resilient system. Therefore, resilience against extreme variations in the environment could be achieved. The concept of CIRLEM, accordingly, is inspired by nature to benefit from the emergence of collective behavior and enable flexibility and cohesion attributes on the demand side in energy systems. CI shows a good performance in building energy systems [35] considering the building energy systems as complex systems. Developing a CI-based control system is highly dependent on defining simple models of local interactions that arise in self-organized patterns that occur in different social behaviors in nature such as insects, fish, and birds [35]. Also, because social animals often face repeated tasks and conditions, learning from the past can improve future collective

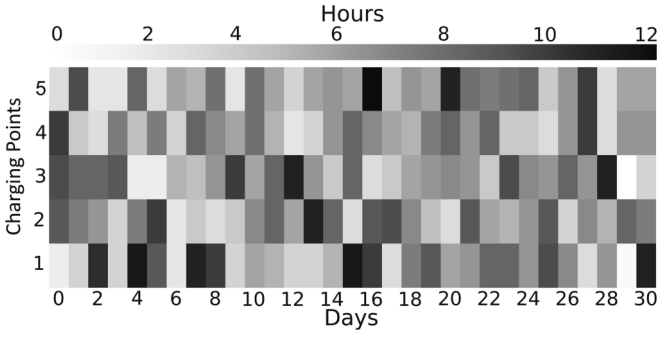

Fig. 4. Heat map of probability of presence of EVs at charging points based on the presence hours in a day for 31 days.

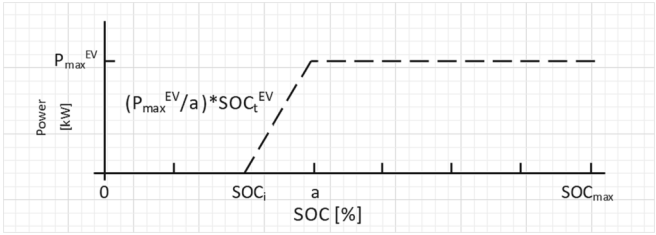

Fig. 5. Power limit for the charging and discharging process in the EV's battery [90].

Table 4
EV characteristics and EV charging points specifications.

EVs and EV charging points specifications	Value
Number of EV charging points	5
Minimum EV energy level	10 %
Maximum EV energy level	80 %
Arrival EV energy level	20 % – 60 %
Max No. of discharge times	2
Maximum charging power	6.6 kW

behavior and enhance decision-making. Collective behavior allows individuals to gain valuable information from collective action when a repeated task is ongoing by the group [93]. Fig. 6 demonstrates the emergence of CI in nature (top) and building energy systems (bottom) in different scales. In a flock of animals, each individual member has a certain level of intelligence to be able to control their behavior and communicate with the neighboring members. This allows them to adjust their action with the overall action in the flock. The behaviors are recognized with simple parameters like speed, direction, and distance so that members can easily understand them, measure them, and apply them consistently. Simple rules are applicable to each behavior (e.g., a certain speed or distance); therefore, exceeding certain thresholds forces the member to adjust its behavior to satisfy the rules. Similar behavior emerges in building energy systems when an individual building/thermal zone is equipped with a smart device to provide intelligence so that the building can adjust its conditions with the overall requirements of the urban area/cluster. Individual buildings are able to modify their conditions by applying adaptation measures, where a certain condition occurs (i.e., rule). Data management and decision-making happen at the individual building level; thus, there is no need for central control, data sharing, and computation.

The key features of CIRLEM (like any other CI-based environment) are applying (1) adaptivity: It is expected that a CI-based energy system is able to adapt its conditions to the extreme climate events, (2) interaction: entities within CIRLEM, including thermal zones and systems, are able to interact to synchronize their need and status upon necessity, and (3) rule: simple rules are defined in the system to enable the adaptivity to react to the environmental variations [47]. Agents/entities have a certain level of intelligence and can control and modify their conditions [94] upon receiving the flexibility signal which governs the system based on the defined rules.

Fig. 7 illustrates the algorithm's components (left) and agents with their adaptation measures (right). Blue square (brain/chipset icon) shows the agents (smart device within the room or equipment), the dashed green line shows the communication flow (signal and demand) between CIRLEM and the agents, solid black lines represent the power supply, dashed black lines show the agent's access to the appliances or equipment within the room for the purpose of control. The adaptation measures are the electronically controllable energy systems in the building that allow the flexibility program to adjust the demand. CIRLEM algorithm is implemented on the EMS in the building where it has the ability to send control commands to the available controls in the thermal zones such as thermostats, and smart plugs (for detailed information see [60]). Therefore, the temperature and ventilation setpoints have to be controlled electronically and be able to receive commands from EMS. Equipment load is controlled by smart plugs that can be on or off through a digital command from EMS, and, finally, EV chargers have

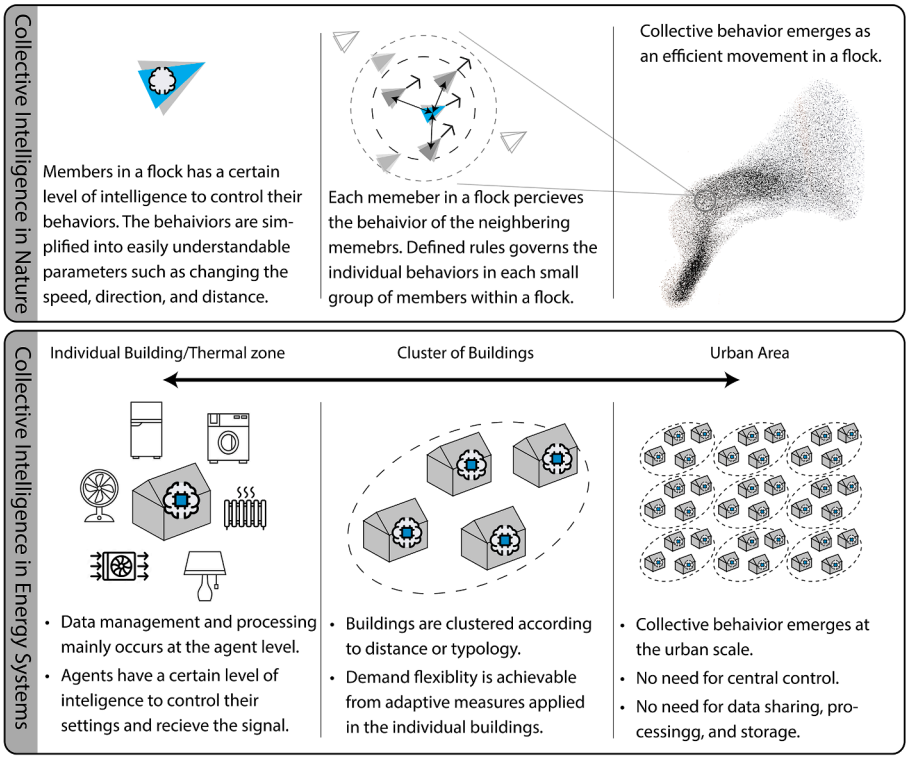

Fig. 6. Collective Intelligence in nature (top) and in energy systems (bottom) representation from individual scales to large scales.

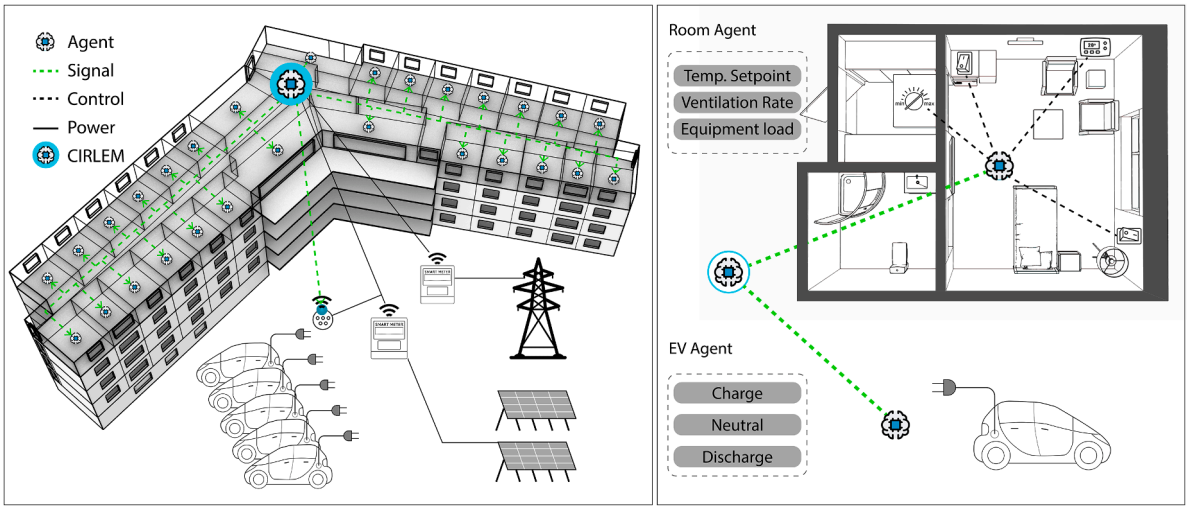

Fig. 7. The components of CIRLEM (left), and agents with their adaptation measures: room (top-right) and EV (bottom-right).

control switches to shift between charge/neutral/discharge. The introduced pilot case is already equipped with these controls showing the possibility and practicality of the solution. Flexibility can be applied in different time scales, from a scale of a few hours to a sub-hourly scale. Studies show that shorter time steps perform better in reacting to variations [35]. In this framework, each room is an agent (110 agents in total), and the EV charging station is also considered an agent. CIRLEM applies a 15-minute time step in controlling and monitoring, to activate the flexibility program. The defined adaptation measures to provide adaptivity and enable flexibility are presented in Table 5.

The control algorithm in CIRLEM utilizes the concept of RL, using a simplified scheme given that RL performs well in distributed and collaborative decision-making strategies [52,53]. Meta-learning was adopted for this work because *meta*-learning or "learning to learn" allows for learning from very limited data and accelerates the learning process by narrowing the possible actions at each time step. Accordingly, the algorithm is divided into two phases: (1) a Decision Tree (DT) and (2) a Watch-Try-Learn (WTL) algorithm. The first step (i.e., DT) uses the metadata which is imported into the process primitively to assist the agent to learn with less information thereafter. The second part (i.e., WTL) is the learning process inspired by RL which is fed by the *meta*-data [95]. The algorithm's workflow is illustrated in Fig. 8.

2.5.1. Phase I: Meta-Learning (Decision Tree)

The DT is implemented at the agent level to learn the common structure (see Zhou et al. [95]) such as time-dependent variables (e.g. TV time, bedtime, lunchtime, weekend schedule, weekday schedule, etc.) and event-based variables (indoor temperature, zone type, occupancy, etc.). The DT could be an empirical flowchart for different conditions in the building (such as day or night, occupied or unoccupied, weekday or weekend, etc.) to represent common rules and conditions. However, a DT can also be generated from observed data [96,97]. The DT, in this work, is developed based on measured electric energy (E), measured outdoor air temperature (T), and timestamps (t). Other weather parameters are removed from the model because they are of less significance in the model based on the P-value test. To generate the DT, a

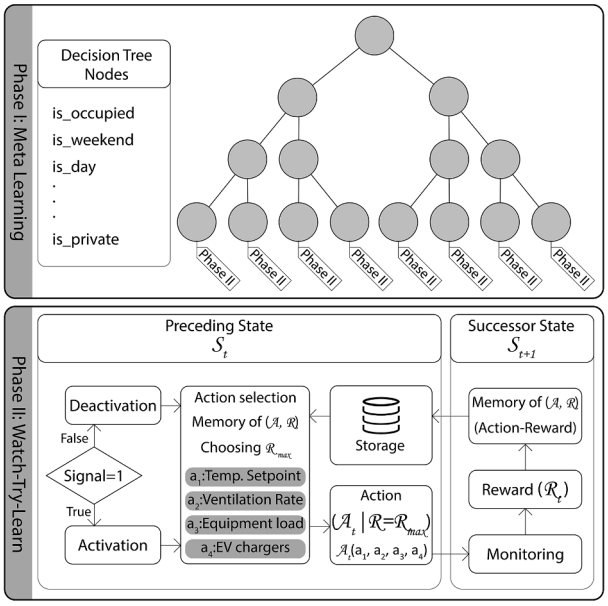

Fig. 8. CIRLEM workflow is divided into two phases: Meta-learning (top) and Watch-Try-Learn (bottom).

Linear Regression Model (LRM) is developed based on E and T. The LRM is analyzed further to add nodes to better fit the regression line into the data point, which gives short lines corresponding to the sections of the data points (i.e., short lines are the broken regression line at each node). Subsequently, the most frequent timestamp (i.e., corresponding to the observations) over each short line is assigned to that short line as the time tag of that (E, T) combination. The time tags are presented in Table 6. Given that the data points at the end of each branch do not

Table 5
Available adaptation measures within the agents.

Agent	Adaptation measure	Values
Room	Temperature setpoint	22, 23, 24, 25, 26, 27 [°C]
	Ventilation rate per floor area	0.1, 0.4, 0.7, 1.0 [l/s/m^2]
	Equipment load	0, 2, 4 [W/m^2]
EV charger	Discharge/Neutral/Charge	−1, 0, 1

Table 6
Time tags for the Decision Tree.

Period	Time	Time tag
Weekly	Mon – Fri	Weekday
	Sat - Sun	Weekend
Daily	06:00–11:00	Morning
	12:00–17:00	Midday
	18:00–21:00	Evening
	22:00–06:00	Night

entirely represent the possible conditions, a complementary algorithm is added as Part II to produce more accurate decisions.

2.5.2. Phase II: Watch-Try-Learn

After identifying the correct branch in DT (the adequate time and event), the WTL component reacts to unseen occurrences. WTL is a Q-learning algorithm which is model-free values-based RL that learns by doing and improve its policy over time in a finite horizon. Q-learning provides the agents to take optimal actions through learning by experiencing the consequences of each action [98]. The WTL component comprises State (S), Action (A), Probability of state-action combinations (P), and Reward (R), which can be denoted by (S, A, P, R) quadruple values. The state represents all the knowledge that the agent has about global conditions. An action is the process of updating the agent conditions toward the goal via available adaptation measures. The reward is immediate feedback based on the system's goal to enhance the system's performance. Given the current state completely characterizes the process, in such an environment this system can be counted as a Markov Decision Process (MDP) [99,100], where Q-learning performs remarkably in solving problems [101]. In an MDP, each state depends on the preceding states, as shown in Eq. (3), where s' is the successor state of s and $p(s', r|s, a)$ is the probability of transition to state s' with reward r, from state s and action a. Additionally, all the parameters in the quadruple values of (S, A, P, R) necessarily have finite numbers of elements, and actions and states interact in discrete time [102].

$$p(s', r|s, a) \doteq \Pr\{S_t = s', R_t = r|S_{t-1} = s, A_{t-1} = a\} \tag{3}$$

In this research, the term state refers to an agent's internal and external conditions, such as energy use, weather, occupancy, etc. A flexibility signal is generated based on the state (i.e., internal, and external conditions) and carries the information to the agents. Therefore, agents are informed and updated via the signal. Agents can act through adaptation measures (see Table 5) which enable agents to modify their conditions by applying or disapplying adaptation measures independently from the whole system. The reward is a function of energy and thermal comfort as improving energy use and maintaining thermal comfort are primary goals of the study. This will be explained in detail in the following section. The CIRLEM's kernel in this research is Edge Node Control (ENC) with a memory length of 24 and 10 % randomness, which are explained in detail in the following sections.

2.5.3. Action

As flexibility is required which is based on the signal received, the algorithm at the agent level selects actions based on the *meta*-learning phase and the rewards obtained in previous experiences. Actions are the changes to conditions made by an agent using available adaptation measures. Actions can be combinations of available adaptation measures at the agent level. Saying that action is a set of values for each zone made of each actuator (see Table 5) which can be denoted as $\{a_1, a_2, a_3\}$ where a_n is the available actuators in the zone; for example, an action can be {22, 0.4, 2} corresponding to {temperature setpoint, ventilation rate, plug load}. Each actuator, according to its current value can obtain a few values at each time step, and the changes are limited in time to avoid large fluctuations in the energy system and disruption in thermal comfort. Specifically, temperature setpoint and ventilation rate can vary maximum of ± 2 steps in values mentioned in Table 5. Also, not all adaptation measures are available at any time because the DT may filter them based on the time or conditions. For example, the plug load in the rooms supplies the fridge with electricity; therefore, there is a constraint that if the fridge is off, it needs to be turned on after a maximum of 3 h and it cannot be turned off before it has run for at least 1 h. Another example is the ventilation rate in public rooms over the weekend when visitors come to the care center. During these times, the algorithm does not change the ventilation rate. Accordingly, there would be different combinations of actions at each timestep. The possible choices, thus, give a 2D array in which each row is a set of actuators or an action like $[\{a_1, a_2, a_3\}, \{a_1', a_2', a_3'\}, \{a_1'', a_2'', a_3''\}]$. As an example, taking {22, 0.4, 2} as the current actuators value in the zone, the possible actions could be [{22, 0.4, 2}, {22, 0.1, 2}, {22, 0.7, 2}, {22, 1.0, 2}, {22, 0.4, 0}, {22, 0.1, 0}, {22, 0.7, 0}, {22, 1.0, 0}] by assigning the values of 22 for temperature setpoint, 0.4, 0.1, 0.7, and 1.0 to ventilation rate, and 0 and 2 for plug loads. The algorithm then seeks in its memory to find the corresponding reward for these actions and chooses the action with the maximum reward unless the choice is random. The agent can also decide randomly in 10 % of the choices to explore all potential actions and avoid binding to limited choices (For more information check [60]).

2.5.4. Reward

According to the definition, reward leads the system to perform better in terms of reaching its goal. The goals of this pilot building study are to elevate grid autonomy and maintain thermal comfort in the defined zone. Agents earn rewards individually based on their performance. To consider grid dependence in the reward, the reduction in purchased electricity is defined by the grid at the current timestep (t) compared to the previous timestep (t-1) as the indicator for electricity performance according to Eq. (4).

The thermal comfort indicator in the reward is calculated using Eq. (5) and is based on whether the operative temperature (T_{opt}) is within the range of comfortable conditions. Standard EN 16798–1 [103] provides guidance in guaranteeing proper indoor thermal comfort conditions for the elderly. It recommends Category I, which presents the narrowest constraints. The building is mechanically cooled in summer; thus, the Fanger model is used. Assuming a metabolic rate of 1 met, which corresponds to a seated, quiet person, a typical summer indoor clothing of 0.5 clo, 60 % relative humidity, and an air speed of 0.1 m/s, the upper thermal comfort limit for indoor operative temperature in summer is 26.3 °C. However, if the occupants are taken as standing, the limit to maintain indoor thermal comfort conditions in Category I is decreased to 25.6 °C, due to a higher average metabolic rate (1.2 met). In this research, the most restricted threshold is used together with the CIBSE overheating criteria [104]. Finally, the reward function is calculated based on Eq.(6).

$$E = \begin{cases} +1 & E^t_{grid} < E^{t-1}_{grid} \\ -1 & E^t_{grid} \geq E^{t-1}_{grid} \end{cases} \tag{4}$$

$$C = \begin{cases} +1 & T_{opt} \text{ within the range} \\ -1 & T_{opt} \text{ outside the range} \end{cases} \tag{5}$$

$$R = \begin{cases} +1 & E > 0 \text{ and } C > 0 \\ 0 & E \leq 0 \text{ or } C \leq 0 \\ -1 & E < 0 \text{ and } C < 0 \end{cases} \tag{6}$$

The reward is an independent value for each agent. Therefore, the calculation may differ slightly between agents. Given that EVs do not contribute to maintaining thermal comfort directly, the comfort indicator (C) is equal to 0 for EVs at all times, and the reward for EVs can be 0 or 1.

2.5.5. Flexibility signal

The flexibility signal (mentioned as "signal" in this work) is a binary value that activates or deactivates the flexibility program. When the signal is 0, the EMS operates as usual. When the signal changes to 1, the flexibility algorithm is activated. It is the EMS that receives the signal from the environment and adopt it to make decisions and send commands to the available controllers/adaptation measures which is certain values and range for each of the controllers (see Table 5). The signal depends on electricity demand in typical and extreme conditions. The typical building electricity demand profile is calculated based on the building energy performance simulation using TDY weather data. The

typical demand equals the seasonal average value, which is that of summer in this case. Thereafter, the electricity use under extreme conditions is calculated at each timestep of the energy performance simulation using EWY weather data (see section 2-2.2). Regardless of whether the total electricity use exceeds the typical baseline, the signal will be 1. Eq. (7) shows the signal values where E_{EWY} is the total electricity use of the building under EWY and $\overline{E}_{TDY}$ stands for the average seasonal electricity use in TDY (For more details see [35]).

$$Signal = \begin{cases} 0 & E_{EWY} \le \overline{E}_{TDY} \\ 1 & E_{EWY} > \overline{E}_{TDY} \end{cases} \quad (7)$$

2.5.6. Memory

After each experience (i.e., iteration in time), CIRLEM stores the set of action-reward (A-R) in the memory to be able to retrieve the actions corresponding to higher rewards. Memory has two important parameters: (1) length and (2) randomness. The length is the number of A-R sets that can be stored which limits the options for choosing, also, it helps to increase the processing speed and convergence. CIRLEM utilizes a memory with a length of 24 which is called ENC-L24. The random behavior is an intrinsic feature of RL letting it explore new choices and not stick to a few early-achieved good options. In this research, CIRLEM applies a random control to the agent with a 10 % probability (more information about the impacts of randomness on the outputs in [60]).

2.6. Thermal comfort

Commonly two approaches are used to assess thermal comfort: the PMV or Fanger model, which is indicated for heated or mechanically cooled buildings, and the adaptive model, which is used for occupant-controlled naturally conditioned spaces or, as introduced in ASHRAE 55–2020 [105], when there is no mechanical cooling system or heating system in operation. These models have already been integrated into several international standards such as ISO 7730 [106], ASHRAE 55 [105], and EN 16798 [103]. In addition, Standard EN 16798:1–2019 defines categories of indoor environmental quality related to probable occupant expectations, providing specific thresholds based on these categories. The standard recommends Category I (which is characterized by the most restrictive constraints among all categories) for spaces occupied by very sensitive and fragile people like the elderly. Beyond providing thermally comfortable environments, it is necessary to ensure occupant health. According to the World Health Organization [107] a lower limit of 20–21 °C in winter should be catered. To control the risk of overheating, the Chartered Institution of Building Services Engineers (CIBSE) has defined the CIBSE [104] overheating criteria, which indicate that there should be no more than "1% annual occupied hours over the operative temperature of 28 °C," which is reduced to 26 °C in bedrooms unless ceiling fans are available. More recently, the guide was updated to incorporate considerations for adaptive comfort models [108].

2.7. Performance evaluation

To assess the algorithm's performance in the pilot case, a scenario is delineated to integrate all the components. The test period is July 2050 under EWY conditions. The signal is calculated based on the average summer (June-July-August) electricity use under TDY (a similar approach was implemented in earlier work [35]). The building operates as usual, the staff work according to typical work schedules, and no holiday is included except weekends. Staff and visitors are allowed to charge their EVs for free if they tend to participate in the flexibility program through the EV agent. It is assumed that cars will leave the charger point with at least 10 % more SOC than the initial value; thus, staff and visitor EVs will not lose charge when parked.

The performance evaluation focuses on (1) energy and (2) thermal comfort. Two indicators are defined to evaluate the energy performance quantitatively, including the Self Consumption Rate (SCR) and Grid Autonomy (GA). The SCR expresses how much energy use is covered by local generation in different consumption and production strategies [109]. Eq. (8) shows the calculation of SCR and GA is calculated through Eq. (9). GA aims to assess how the building withstands a power outage or high electricity price by applying the proposed control algorithm.

$$SCR = \frac{\sum_{d=1}^{n_d}\sum_{t=1}^{24}\left(P_{PV}^{(d,t)} + SOC_{EV}^{(d,t)}\right)\Delta t}{\sum_{d=1}^{n_d}\sum_{t=1}^{24}\left(P_{load}^{(d,t)}\right) \bullet \Delta t} \quad (8)$$

$$GA = \frac{n\left(\left\{t | P_{grid}^{(t)} = 0\right\}\right)}{n(h) \bullet \Delta t} \bullet 100 \quad (9)$$

To ensure adequate indoor thermal comfort conditions, the Fanger comfort model is applied to the control algorithm. All zones are considered as Category I and the temperature thresholds of 23.5 °C and 25.6 °C are set as constraints for indoor operative temperature [110]. In addition, the temperature ramps, which are defined as actively controlled operative temperature changes, are investigated with respect to the limits defined in ASHRAE 55–2020 [105]. The evaluation is carried out in 15, 30, and 60 min based on the denoted limits in Table 7.

The evaluation follows three scenarios as follows:

- TDY-noCIRLEM: Under TDY conditions with regular operation without implementing CIRLEM
- EWY-noCIRLEM: Under EWY conditions with regular operation without implementing CIRLEM
- EWY-CIRLEM: Under EWY conditions with CIRLEM in operation

Comparison between these scenarios will produce an understanding of how the building would perform in typical future weather (TDY-noCIRLEM), whether it would tolerate extreme warm conditions (EWY-noCIRLEM), and finally, assess the performance of the algorithm in coping with extreme climate conditions (EWY-CIRLEM). Afterward, the impacts of adding PV and EV to the system are assessed.

3. Results and discussions

This chapter presents the results and analysis of CIRLEM performance. First, the calibration indicator values are discussed, and then the performance of CIRLEM is presented. In the latter, the building performance with CIRLEM is compared to its regular operations (i.e., without CIRLEM) under typical and extreme climate conditions, without on-site generation and storage (EWY-noCIRLEM vs EWY-CIRLEM). Finally, the results of including of the PV (EWY-CIRLEM:PV) and EV charging stations (EWY-CIRLEM-PVEV) in CIRLEM are presented.

3.1. Calibration of the energy model

The calibration process was carried out first, for a period of one year based on hourly electricity demand, and secondly, for a period of 1 month based on hourly intervals of indoor temperatures. Table 8 presents the values of the calibration indicators over the 1-year period for the electricity demand, 1 month period in July (n = 744) for indoor temperature, and PV production over July. The values of CV(RMSE) and NMBE are within the acceptable range according to ASHRAE Guideline 14 [83].

Table 7
Maximum allowed temperature ramps according to ASHRAE 55–2020.

Time Step [minutes]	15	30	60
Maximum operative temperature changes allowed [°C]	1.1	1.77	2.2

Table 8
Calibration indicators values for BEM and PV modeling.

	Calibration data	CV(RMSE) [%]	NMBE [%]
BEM	Annual electricity demand (n = 8760 h)	15	2
BEM	July indoor temperature (n = 744 h)	15	0
PV	July PV production (n = 744 h)	5	0

3.2. CIRLEM performance

This section presents the results and findings from implementing CIRLEM. This section investigates the algorithm's performance, first, regarding the total electricity demand (demand response), and second, with respect to local generation (PV) and storage (EV).

3.2.1. CIRLEM and energy performance

This section presents the outputs related to the building energy performance including total electricity demand and peak power. In different scenarios, we investigate the demand profile under different weather conditions. The simulated electric energy use for three scenarios is presented in Fig. 9. The values are presented in high temporal resolution using 15-minute timesteps to avoid eliminating changes on the sub-hourly scale. The line graph (left) shows the fluctuations in simulated electric energy use over the analysis period (i.e., July 2050). The boxplots (right) show the distribution of the values in 15-minute timesteps.

TDY-noCIRLEM (green line) shows the energy performance of the building in typical conditions. This can be considered a baseline to better understand how extreme conditions stress energy systems given demand and peak power usage. This curve is also used as the baseline to generate the signal; the mean value of simulated electric energy use in TDY-noCIRLEM is the reference value to generate the signal (see 2.5.5). EWY-noCIRLEM (the gray dashed line) shows the building performance under extreme climate conditions without using CIRLEM which indicates the simulated energy performance if CIRLEM is not deployed under extreme events. Finally, EWY-CIRLEM (the red line) indicates the performance of CIRLEM. TDY-noCIRLEM (the green boxplot), which conveys the results under typical conditions without CIRLEM, shows a maximum of 25 kW, while this can reach up to approximately 72 kW under EWY-noCIRLEM (the gray boxplot), in extreme conditions and without CIRLEM. Where CIRLEM was applied, EWY-CIRLEM (the red boxplot), peak power could be reduced by 26 % to 57 kW. In typical conditions (TDY-noCIRLEM) the building is expected to experience a demand of 11.3 MWh in July. The extreme weather conditions (EWY-noCIRLEM) may increase the demand to 27.5 MWh, and by applying CIRLEM the total demand (EWY-CIRLEM) could be reduced to 18.1 MWh over the month with 35 % reduction. Over this period (2976 timesteps) signal-1 s were generated 1260 times and transmitted to the agents (42 % signal-1 and 58 % signal-0). The line graph shows that in the 3rd and 4th weeks of July there were considerably extreme climate conditions. Therefore, this period was selected for further analysis in finer resolution.

An investigation of the two-week period with the highest demand in July was performed and the results are presented in Fig. 10. The graph on the left shows the electricity use for three scenarios. The signal is presented at the top as a 0 or 1 value (white/blue). In total, 840 signal-1 s were transmitted to the agents among 1344 timesteps over the two-week period which was roughly 62 % of all signals. Compared to the entire month, 66 % of all signal-1 s were generated in these 14 days showing a higher necessity for flexibility in this period. The difference between EWY-noCIRLEM (the dashed gray line) and EWY-CIRLEM (the red line) shows the load curtailment at each timestep. Particularly on days of higher demand, such as the 19th, 24th, and 25th, CIRLEM flattened the energy demand profile by up to 20 kW in the middle of the days from around 11:00 to 16:00. As expected, signal-1 was transmitted mostly during the day as higher outdoor temperatures and solar radiation increased the demand for cooling and ventilation.

3.2.2. CIRLEM and grid electricity

This section presents the outputs and discussions of CIRLEM including PV and EV, and focuses on the effects of on-site generation and storage on the volume of electricity delivered from the grid. To investigate the performance of distributed generation and storage in collaboration with the demand response (which refers to EWY-CIRLEM scenario), two sub-scenarios for EWY-CIRLEM were introduced: (1) EWY-CIRLEM:PV and (2) EWY-CIRLEM:PVEV. According to the findings from the previous section, signal-1 was transmitted primarily in diurnal hours, which provides preemptive support for the proposal of using the EVs as the storage side. This can enhance the flexibility of the system and provide a degree of grid autonomy. EWY-CIRLEM-PV adds PV to CIRLEM as an on-site supply source. However, PV was not an agent itself since CIRLEM does not control it and there was no adaptation measure for PV in the algorithm. The impact of PV appears on EVs' SOC and as an agent it earns rewards for taking actions. EVs are charged only by PV production, not the grid, and have three modes: charge, discharge, and neutral. The EWY-CIRLEM-PVEV scenario was developed to include the EV charging station as an agent of CIRLEM to create on-site storage. The grid electricity was calculated from $GridEl. = P^t_{load} - P^t_{PV} - P^t_{storage}$ where $P^t_{storage}$ was taken as the power supplied by the EVs. In EWY-CIRLEM:PV, $P^t_{storage}$ was equal to 0 as there were no EVs in the system.

Fig. 11 shows the simulated electric energy for EWY-CIRLEM:PV (in

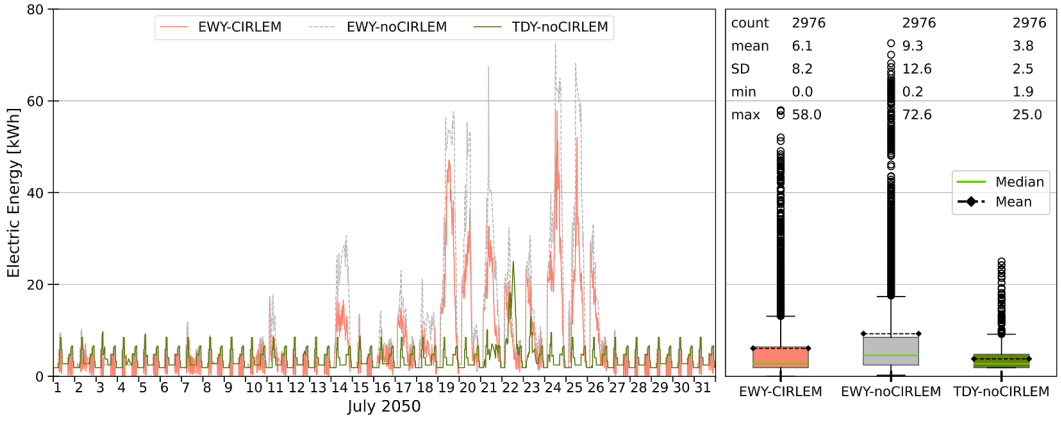

Fig. 9. Simulated electric energy use over a period of one month (July 2050) for EWY-CIRLEM (red), EWY-noCIRLEM (dashed gray), TDY-noCIRLEM (green): hourly profiles (left), and boxplots with major statistical values (right).

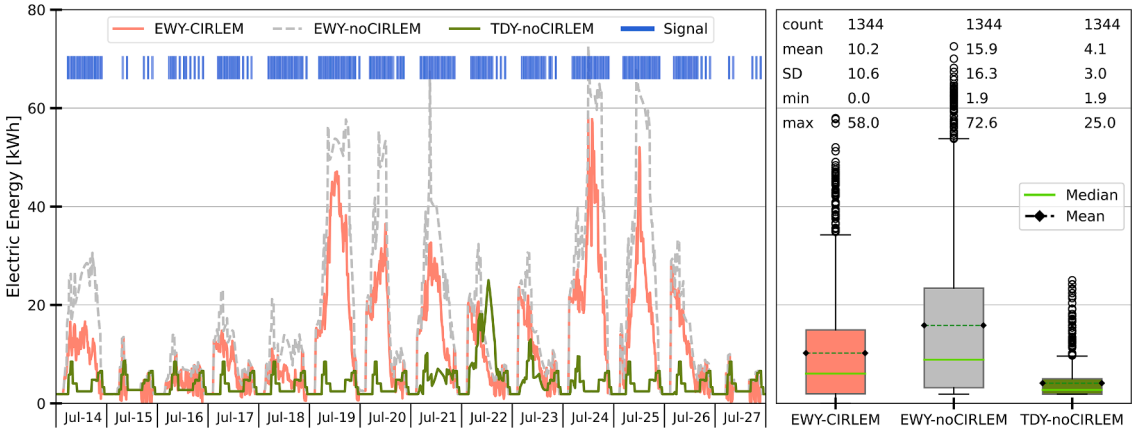

Fig. 10. Simulated electric energy use over two weeks with the highest demand in July 2050 for EWY-CIRLEM (red), EWY-noCIRLEM (dashed gray), TDY-noCIRLEM (green): hourly profiles and flexibility signal (blue) (left) and boxplots with major statistical values (right).

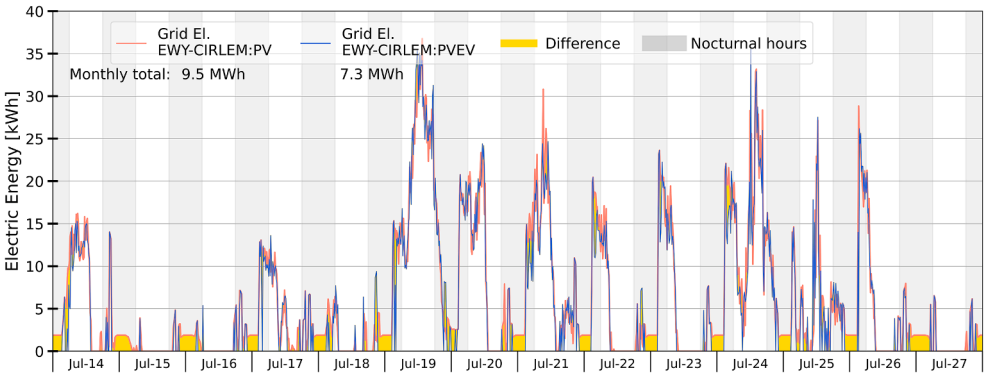

Fig. 11. Simulated electric energy from the grid for EWY-CIRLEM:PV (red) and EWY-CIRLEM:PVEV (blue) over two weeks (from 14th to 17th July). The solid yellow shows the difference between the two scenarios. The gray fade strips point out the nocturnal hours from 18:00 to 06:00.

red) which equals the building load minus electricity supplied by the PV station at each timestep. EWY-CIRLEM:PVEV (in dark red) shows the electricity purchased from the grid (i.e., the load covered by the grid) when the system used the stored electricity in the on-site storage (i.e., EVs). The yellow fade shows the difference between the two profiles which resulted from the storage. As expected, the impact of utilizing the storage appears mostly during nights when there is no PV production. The total supplied electricity from the grid without storage (EWY-CIRLEM:PV) was 9.5 MWh while adding the storage (EWY-CIRLEM:PVEV) reduced grid electricity usage by around 25 %, to 7.2 MWh. The difference (2.3 MWh) was provided by the stored PV production.

The PV station produced 18.9 MWh over the analysis period, and the building's electricity demand was equal to 18.1 MWh. However, the building demand was not entirely covered by PV production due to the demand and production mismatch. According to Fig. 11, applying EWY-CIRLEM:PVEV covered 10.9 MWh of the total demand, giving a value of grid electricity equal to 7.2 MWh (18.1 −10.9). The remainder of the PV production equaled 8.4 MWh (18.8 −10.9) which was used to charge the EVs. This PV production excess can be considered as an encouragement for EV owners to participate in flexibility, encouraging adherence to best practices regarding when and for how long to plug the car in. Therefore, building and EV owners could be encouraged to participate in this mutually beneficial arrangement.

To investigate how much of the electricity demand on-site generation could cover, the self-consumption rate was deployed. In EWY-noCIRLEM the value of SCR was equal to 68 %. This value increased to more than 100 % by applying CIRLEM in the building with a maximum value of 132 % when utilizing EVs (EWY-CIRLEM:PVEV). The values of grid autonomy were equal to 30 %, 41 %, and 69 % for EWY-noCIRLEM, EWY-CIRLEM:PV, and EWY-CIRLEM:PVEV, respectively, as presented in Table 9. Adding PV and EVs to the building energy system can reap significant benefits for grid autonomy.

Further investigation was carried out on grid autonomy using the hourly values for EWY-CIRLEM:PV and EWY-CIRLEM:PVEV. The results are shown in Fig. 12. The values on the horizontal axis represent hours of the day containing the total number of timesteps (15-minutes in length) with grid autonomy in each hour over the analysis month (each hour refers to 124 (31*4) values for the correlated hour in July). For instance, number 13 (13:00) refers to all the 13:00 s in 31 days of the month with sub-hourly (13:00, 13:15, 13:30, 13:45) values. The percentage on the vertical axis is the ratio of timesteps with grid autonomy to the total timesteps (31*4 = 124), where, for example, at hour 2, around 81 % of timesteps are independent of the grid in EWY-CIRLEM:PVEV (the blue line).

The percentage of GA in EWY-CIRLEM:PV was around 0 % after midnight until morning while this value increased to around 70 % in the middle of the day due to day-time PV production. Adding the storage (EWY-CIRLEM:PVEV) raised grid autonomy significantly between midnight (0:00) and early morning (5:00–6:00) from 0 % to 60 %-80 %

Table 9
SCR and GA values for EWY-CIRLEM.

Scenario	SCR [%]	GA [%]
EWY-noCIRLEM	68	30
EWY-CIRLEM:PV	104	41
EWY-CIRLEM:PVEV	132	69

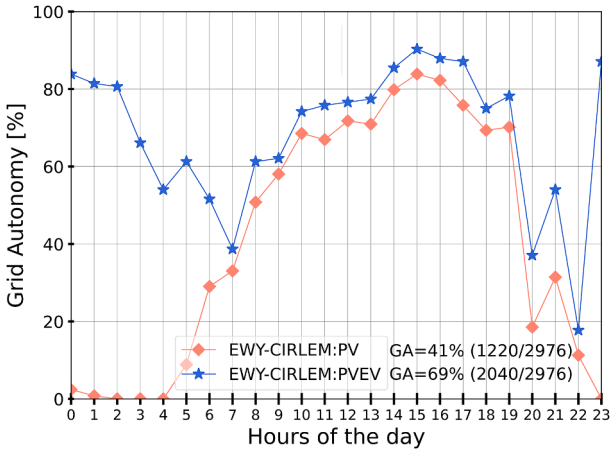

Fig. 12. The percentage of timesteps with grid autonomy among all timesteps (24*4*31) over the analysis period (July) for EWY-CIRLEM:PV (red) and EWY-CIRLEM:PVEV (blue). Each hour contains sub-hourly (15-minute) values referring to the hour in all 31 days of the analysis period.

due to the stored electricity from the day before in the EVs plugged in overnight. During the day, the value increased by approximately 7 % each hour.

In total, PV meant that for almost 41 % of the hours simulated, the building was independent of the grid, and when EV storage was added this increased to approximately 69 % of the whole period. The sharp decrease of the GA value between 4:00 and 7:00 in EWY-CIRLEM:PVEV was caused by reductions in the state of charge (SOC) of EVs after several hours without PV production while the demand was growing at the beginning of the day. The relatively constant difference between the red and blue curves shows the availability of electricity from EVs for almost the entirety of the day when PVs generated electricity. This demonstrated the potential performance of the independent decision-making of EVs as an agent, influenced by rewards earned.

As mentioned before, on-site generation was more than the defined EV capacity. Thus, there is still potential to increase the GA value by increasing the EV capacity. The EV capacity could grow further through greater participation among local people, employees, and visitors. Monetizing solutions and incentives may also increase participation. Indeed, an accurate analysis of the electricity price should be carried out given that in Norway, the dynamic pricing system is applied on an hourly scale with considerable differences between day and night. However, this study has aimed to increase resilience under extreme weather conditions, and the economic aspects were deferred.

3.2.3. *CIRLEM and indoor thermal comfort*

Given the stated aims of this research, namely, to facilitate the maintenance of proper indoor thermal comfort conditions for vulnerable residents while enhancing energy performance, in this section, the operative temperature variations in the indoor environment are analyzed. Fig. 13 illustrates the distribution of indoor temperatures under the scenario EWY-CIRLEM (in red), EWY-noCIRLEM (in gray), TDY-noCIRLEM (in green), and measured values registered in July 2022 (in dark gray). The simulated values refer to 110 thermal zones (i.e., 110 zones × 31 days × 24 h × 4 timesteps/hour) while historic values correspond to the four sample rooms (i.e., 4 zones × 31 days × 24 h). Given that CIRLEM seeks the temperature thresholds for the Fanger comfort model based on EN 16798–2:2019 [110], the upper and lower thresholds are visualized on the graph (the red lines).

The historic measured values show that the indoor temperature was always within the recommended upper limit with a mean value of 23.9 °C, a minimum of 21.5 °C, and a maximum of 25 °C. Under a typical future climate (TDY-noCIRLEM), overheating would occur with only 0.5 h •°C per zone during the entire month. However, extreme

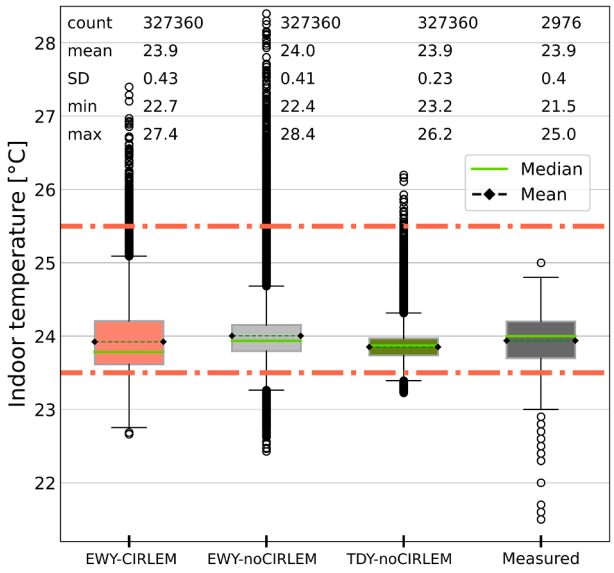

Fig. 13. Indoor air temperature distribution for EWY-CIRLEM (red), EWY-noCIRLEM (gray), TDY-noCIRLEM (green) including 110 zones, and measured values in July 2022 (dark gray) including 4 zones. Red lines show the thresholds for indoor temperature based on the Fanger thermal comfort model. Major statistical values are denoted on top.

conditions did increase the overheating to 17 h •°C per zone over a month when CIRLEM was not in operation. Adding CIRLEM into the building could reduce overheating under extreme conditions (EWY-CIRLEM) to 2 h •°C per zone during the entire month. It is important to consider that these values are not distributed evenly between the zones. The sub-scenarios of EWY-CIRLEM were subject to the same impacts on the demand profile and indoor conditions; hence, they were not investigated separately. As CIRLEM modified the temperature setpoint continuously, there is a risk for indoor temperature fluctuation which could disturb indoor comfort conditions. The temperature ramps are assessed to verify that the rate of change in operative temperature does not exceed comfort acceptability, as indicated in ASHRAE 55–2020 [105]. Fig. 14 shows the temperature variations at each timestep with

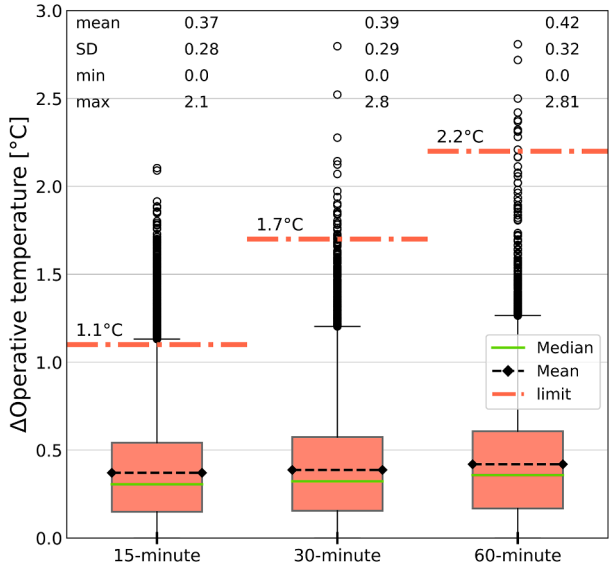

Fig. 14. Indoor operative temperature variations in 15-minute, 30-minute, and 60-minute timesteps in all the zones over the analysis period. Data is related to EWY-CIRLEM. The overall statistical descriptions are denoted on the top of each boxplot.

15-, 30-, and 60-minute intervals in all the zones. The box plot shows the absolute values of the temperature variations in °C (i.e., $|(T_{t2} - T_{t1})| \bullet \Delta t$, $\Delta t \in \{15', 30', 60'\}$) for EWY-CIRLEM where the dashed dotted red lines indicate the ASHRAE 55–2020 limits for the temperature ramps.

In the 15-minute timestep, the mean value was 0.38 °C, and the interquartile range lay between 0.15 °C and 0.55 °C. The outliers show temperature variations from 1.15 °C up to around 2.05 °C. The temperature variations in the 15-minute timestep exceeded the limit for less than 2 % of the time in all the zones. In the 30-minute timesteps, the mean value was equal to 0.40 °C where the upper quartile lay at 1.20 °C. In this case, around 0.1 % of the time the temperature variations exceeded the limit. The hourly timestep (60-minute) showed a mean value of 0.43 °C while the upper quartile was equal to 1.27 °C. The temperature variation in the hourly time span almost did not exceed the limit (i.e., less than 0.02 % of the time). Accordingly, the defined constraints for the adaptation measures could maintain the indoor temperature with acceptable variations.

3.3. Future Development

Future work is ongoing in two main branches. The first one is performance evaluation in winter under extreme cold conditions. The second one is to develop the functioning algorithm for CIRLEM at the cluster level where several buildings are included in the EM. This requires a higher level of decision-making to coordinate different buildings with different owners, preferences, and characteristics. After all, CIRLEM is to be applied in a real case to evaluate the performance in real conditions. In this case, it is possible to evaluate how is the performance with a low amount of data sharing and computation power when CIRLEM is running on a small service equipped with a single-board computer. According to the results of this simulation-based research, an experiment is ongoing to deploy CIRLEM in a real case with regular operation under extreme conditions.

4. Conclusion

Climate change affects the aged population with more pronounced effects, especially under extreme events. The United Nations (UN) Sustainable Development Goals (SDG) emphasize the resilience of cities and ensuring well-being for all residents of all ages. Accordingly, the UN defines adaptability as an essential need to achieve resilience. Energy flexibility, therefore, plays a significant role in providing resilience in energy systems where building can adapt their demand and production based on the users' needs and grid requirements. Maintaining thermal comfort is a vital role of buildings which is highly dependent on energy systems, which, in the case of failure, may cause severe health issues for the occupants especially vulnerable groups of people.

CIRLEM is an Energy Management (EM) algorithm based on Collective Intelligence (CI) integrated with Reinforcement Learning (RL). This research proposes a novel structure for CIRLEM to coordinate demand-, generation-, and storage-side in building energy systems deploying a learning process in two stages: (1) Meta-learning, and (2) Watch-Try-Learn (WTL). The first stage helps to accelerate the second layer which is a simplified model-free Reinforcement Learning (RL) algorithm. The aim is to reduce the computational demand and data required for decision-making without the need for data gathering and sharing such as data for weather conditions, building models, or user behaviors. The algorithm applies the logic of action-reward where the flexibility is enabled by a signal. The signal is generated based on the typical energy demand as the baseline. The algorithm is based on the independent agents in the system which could control their conditions autonomously through CIRLEM. Agents are equipped with adaptation measures and sensors to control the energy systems and monitor conditions, respectively. Therefore, agents could modify their conditions independently based on the rewards earned. In this research, agents are defined as private rooms, public rooms, offices, and EV chargers. The adaptation measures are temperature setpoint, ventilation setpoint, plug loads for the rooms, and charging or discharging for the EV charging points.

The research investigates the variation of energy use and indoor conditions in an elderly care center in Ålesund, Norway during summer considering typical and extreme warm conditions to evaluate the effectiveness of the proposed control approach under future climate conditions. The case study uses a newly constructed building fully equipped with the Energy Management System (EMS). In addition, there is a roof-top Photo Voltaic (PV) station and a low-current Electric Vehicle (EV) charging station. To evaluate the performance of the algorithm, monthly energy demand and peak power, Self-Consumption Rate (SCR), and Grid Autonomy (GA) are taken into the account.

The results of the dynamic energy simulations show that the implementation of CIRLEM can significantly decrease energy use under the assumption of extreme weather conditions, while guaranteeing proper indoor thermal comfort conditions, even during temperature ramps. Specifically, applying CIRLEM under extreme warm conditions could reduce the energy demand by around 35 % and peak power by 26 %. Deploying CIRLEM can increase SCR and GA from 68 % to 132 % and 30 % to 69 %, respectively. The assessment of indoor thermal comfort shows that the indoor temperature stays within the accepted limits and the temperature ramps in 15-, 30-, and 60-minute timesteps meet the necessary criteria.

Further research is required to extend the investigation to the winter while exploring, in more detail, the potential of combining different CIRLEM strategies. Moreover, the function of CIRLEM in real buildings and running on a smart device (i.e., a single board computer) is ongoing to prove the performance with low data sharing and computation power.

CRediT authorship contribution statement

Mohammad Hosseini: Writing – original draft, Visualization, Software, Methodology, Formal analysis, Data curation, Conceptualization. **Silvia Erba:** Writing – review & editing, Funding acquisition, Formal analysis, Conceptualization. **Parisa Hajialigol:** Writing – original draft, Software. **Mohammadreza Aghaei:** Project administration, Funding acquisition. **Amin Moazami:** Writing – review & editing, Supervision, Project administration, Funding acquisition, Conceptualization. **Vahid M. Nik:** Writing – review & editing, Supervision, Software, Methodology, Funding acquisition, Conceptualization.

Declaration of competing interest

The authors declare that they have no known competing financial interests or personal relationships that could have appeared to influence the work reported in this paper.

Data availability

The authors do not have permission to share data.

Acknowledgment

This work was supported by the European Union's Horizon 2020 research and innovation programme under grant agreement for the COLLECTiEF (Collective Intelligence for Energy Flexibility) project (grant agreement ID: 101033683) and the joint programming initiative 'ERA-Net Smart Energy Systems' with support from the European Union's Horizon 2020 research and innovation programme under grant agreement 108807 for the DigiCiti project.

References

[1] H.-O. Pörtner *et al.*, "IPCC, 2022: Climate Change 2022: Impacts, Adaptation, and Vulnerability. Contribution of Working Group II to the Sixth Assessment Report of

the Intergovernmental Panel on Climate Change," *Camb. Univ. Press Camb. Univ. Press Camb. UK N. Y. NY USA*, p. 3056, doi: 10.1017/9781009325844.
[2] A. Moazami, S. Carlucci, V.M. Nik, S. Geving, Towards climate robust buildings: an innovative method for designing buildings with robust energy performance under climate change, Energy Build. 202 (Nov. 2019) 109378, https://doi.org/10.1016/j.enbuild.2019.109378.
[3] R. Ruuhela, A. Votsis, J. Kukkonen, K. Jylhä, S. Kankaanpää, A. Perrels, Temperature-related mortality in Helsinki compared to its surrounding region over two decades, with special emphasis on intensive heatwaves, Atmosphere 12 (1) (2021) pp, https://doi.org/10.3390/atmos12010046.
[4] S.E. Perkins-Kirkpatrick, P.B. Gibson, Changes in regional heatwave characteristics as a function of increasing global temperature, Sci. Rep. 7 (1) (2017) pp, https://doi.org/10.1038/s41598-017-12520-2.
[5] J. Tollefson, Earth's hottest month: these charts show what happened in july and what comes next, Nature (Aug. 2023), https://doi.org/10.1038/d41586-023-02552-2.
[6] "IPCC, 2019: Summary for Policymakers. In: Climate Change and Land: an IPCC special report on climate change, desertification, land degradation, sustainable land management, food security, and greenhouse gas fluxes in terrestrial ecosystems [P.R. Shukla, J. Skea, E. Calvo Buendia, V. Masson-Delmotte, H.- O. Pörtner, D. C. Roberts, P. Zhai, R. Slade, S. Connors, R. van Diemen, M. Ferrat, E. Haughey, S. Luz, S. Neogi, M. Pathak, J. Petzold, J. Portugal Pereira, P. Vyas, E. Huntley, K. Kissick, M. Belkacemi, J. Malley, (eds.)]. In press.".
[7] X. Hu, et al., Changes in multiple ecosystem services and their influencing factors in nordic countries, Ecol. Indic. 146 (2023), https://doi.org/10.1016/j.ecolind.2022.109847.
[8] Accessed: Feb. 17 (2023) [Online]. Available: https://ec.europa.eu/eurostat/statistics-explained/index.php?title=Ageing_Europe_-_statistics_on_population_developments.
[9] Un,, Transforming our world: the 2030 agenda for sustainable development.: sustainable development knowledge platform [Online]. Available: Accessed (Sep. 20, 2021.) https://sustainabledevelopment.un.org/post2015/transformingourworld/publication.
[10] A.T.D. Perera, K. Javanroodi, V.M. Nik, Climate resilient interconnected infrastructure: co-optimization of energy systems and urban morphology, Appl. Energy 285 (2021), https://doi.org/10.1016/j.apenergy.2020.116430.
[11] S. Erba, A. Barbieri, Retrofitting buildings into thermal batteries for demand-side flexibility and thermal safety during power outages in winter, Energies vol. 15, no. 12, Art. no. 12 (Jan. 2022), https://doi.org/10.3390/en15124405.
[12] H. Haes Alhelou, M.E. Hamedani-Golshan, T.C. Njenda, P. Siano, A survey on power system blackout and cascading events: research motivations and challenges, Energies vol. 12, no. 4, Art. no. 4 (Jan. 2019), https://doi.org/10.3390/en12040682.
[13] A.T.D. Perera, V.M. Nik, D. Chen, J.-L. Scartezzini, T. Hong, Quantifying the impacts of climate change and extreme climate events on energy systems, Nat. Energy 5 (2) (2020) 150–159, https://doi.org/10.1038/s41560-020-0558-0.
[14] V.M. Nik, A.T.D. Perera, D. Chen, Towards climate resilient urban energy systems: a review, Natl. Sci. Rev. 8 (nwaa134) (Mar. 2021), https://doi.org/10.1093/nsr/nwaa134.
[15] A. Dimoudi and S. Zoras, "The Role of Buildings in Energy Systems," 2016, pp. 37–62. doi: 10.1007/978-3-319-20831-2_3.
[16] F. Wiese, Resilience thinking as an interdisciplinary guiding principle for energy system transitions, Resources vol. 5, no. 4, Art. no. 4 (Dec. 2016), https://doi.org/10.3390/resources5040030.
[17] J. Jasiūnas, P.D. Lund, J. Mikkola, Energy system resilience – a review, Renew. Sustain. Energy Rev. 150 (Oct. 2021) 111476, https://doi.org/10.1016/j.rser.2021.111476.
[18] A. T. D. Perera *et al.*, "Challenges resulting from urban density and climate change for the EU energy transition," *Nat. Energy*, vol. 8, no. 4, Art. no. 4, Apr. 2023, doi: 10.1038/s41560-023-01232-9.
[19] A. Moazami, S. Carlucci, S. Geving, Robust and resilient buildings: a framework for defining the protection against climate uncertainty, IOP Conf. Ser. Mater. Sci. Eng. 609 (Oct. 2019) 072068, https://doi.org/10.1088/1757-899X/609/7/072068.
[20] S. Attia, et al., Resilient cooling of buildings to protect against heat waves and power outages: key concepts and definition, Energy Build. 239 (May 2021) 110869, https://doi.org/10.1016/j.enbuild.2021.110869.
[21] S. Zhou, S. Cao, Energy flexibility and viability enhancement for an ocean-energy-supported zero-emission office building with respect to both existing and advanced utility business models with dynamic responsive incentives, Energy Rep. 8 (Nov. 2022) 10244–10271, https://doi.org/10.1016/j.egyr.2022.08.005.
[22] C. Hughes, S. Natarajan, C. Liu, W.J. Chung, M. Herrera, Winter thermal comfort and health in the elderly, Energy Policy 134 (Nov. 2019) 110954, https://doi.org/10.1016/j.enpol.2019.110954.
[23] C.A. Alves, D.H.S. Duarte, F.L.T. Gonçalves, Residential buildings' thermal performance and comfort for the elderly under climate changes context in the city of São Paulo, Brazil, Energy Build. 114 (Feb. 2016) 62–71, https://doi.org/10.1016/j.enbuild.2015.06.044.
[24] Y. Wu, et al., Age differences in thermal comfort and physiological responses in thermal environments with temperature ramp, Build. Environ. 228 (Jan. 2023) 109887, https://doi.org/10.1016/j.buildenv.2022.109887.
[25] J. Younes, M. Chen, K. Ghali, R. Kosonen, A.K. Melikov, N. Ghaddar, A thermal sensation model for elderly under steady and transient uniform conditions, Build. Environ. 227 (Jan. 2023) 109797, https://doi.org/10.1016/j.buildenv.2022.109797.
[26] Y. Jiao, Y. Yu, H. Yu, F. Wang, The impact of thermal environment of transition spaces in elderly-care buildings on thermal adaptation and thermal behavior of the elderly, Build. Environ. 228 (Jan. 2023) 109871, https://doi.org/10.1016/j.buildenv.2022.109871.
[27] Q. Zhao, Z. Lian, D. Lai, Thermal comfort models and their developments: a review, Energy Built Environ. 2 (1) (Jan. 2021) 21–33, https://doi.org/10.1016/j.enbenv.2020.05.007.
[28] T. Ma, J. Xiong, Z. Lian, A human thermoregulation model for the chinese elderly, J. Therm. Biol. 70 (Dec. 2017) 2–14, https://doi.org/10.1016/j.jtherbio.2017.08.002.
[29] C. Hughes, S. Natarajan, Summer thermal comfort and overheating in the elderly, Build. Serv. Eng. Res. Technol. 40 (4) (Jul. 2019) 426–445, https://doi.org/10.1177/0143624419844518.
[30] M.B. Tobey, R.B. Binder, T. Yoshida, Y. Yamagata, Urban systems design case study: Tokyo's sumida ward, Smart Cities 2 (4) (2019) 453–470, https://doi.org/10.3390/smartcities2040028.
[31] C. Serena, Complex adaptive systems, Camb. MA USA 31 (2001).
[32] L.A. Tamberg, J. Heitzig, J.F. Donges, A modeler's guide to studying the resilience of social-technical-environmental systems, Environ. Res. Lett. 17 (5) (2022) pp, https://doi.org/10.1088/1748-9326/ac60d9.
[33] S. Jackson, "Resilience Principles for the ICT Sector," in *Critical Information Infrastructure Protection and Resilience in the ICT Sector*, 2013, pp. 36–49. doi: 10.4018/978-1-4666-2964-6.ch002.
[34] L.D. Gitelman, T.B. Gavrilova, M.V. Kozhevnikov, Methodologies for managing complex systems under uncertainty, WIT Trans. Ecol. Environ. 241 (2020) 91–103, https://doi.org/10.2495/SDP200081.
[35] V.M. Nik, A. Moazami, Using collective intelligence to enhance demand flexibility and climate resilience in urban areas, Appl. Energy 281 (2021), https://doi.org/10.1016/j.apenergy.2020.116106.
[36] A.T.D. Perera, V. Nik, U. Wickramasinghe, J.-L. Scartezzini, Redefining energy system flexibility for distributed energy system design, Appl. Energy 253 (Jul. 2019), https://doi.org/10.1016/j.apenergy.2019.113572.
[37] R. Li, et al., Ten questions concerning energy flexibility in buildings, Build. Environ. 223 (Sep. 2022) 109461, https://doi.org/10.1016/j.buildenv.2022.109461.
[38] S.Ø. Jensen, et al., IEA EBC annex 67 energy flexible buildings, Energy Build. 155 (Nov. 2017) 25–34, https://doi.org/10.1016/j.enbuild.2017.08.044.
[39] H. Li, Z. Wang, T. Hong, M.A. Piette, Energy flexibility of residential buildings: a systematic review of characterization and quantification methods and applications, Adv. Appl. Energy 3 (Aug. 2021) 100054, https://doi.org/10.1016/j.adapen.2021.100054.
[40] L. Luttenberger Marić, H. Keko, M. Delimar, The role of local aggregator in delivering energy savings to household consumers, Energies vol. 15, no. 8, Art. no. 8 (Jan. 2022), https://doi.org/10.3390/en15082793.
[41] H. Tang, S. Wang, H. Li, Flexibility categorization, sources, capabilities and technologies for energy-flexible and grid-responsive buildings: state-of-the-art and future perspective, Energy 219 (Mar. 2021) 119598, https://doi.org/10.1016/j.energy.2020.119598.
[42] F. Pallonetto, M. De Rosa, F. D'Ettorre, D.P. Finn, On the assessment and control optimisation of demand response programs in residential buildings, Renew. Sustain. Energy Rev. 127 (Jul. 2020) 109861, https://doi.org/10.1016/j.rser.2020.109861.
[43] Y. Fu, Z. O'Neill, J. Wen, A. Pertzborn, S.T. Bushby, Utilizing commercial heating, ventilating, and air conditioning systems to provide grid services: a review, Appl. Energy 307 (Feb. 2022) 118133, https://doi.org/10.1016/j.apenergy.2021.118133.
[44] A.T.D. Perera, T. Hong, Vulnerability and resilience of urban energy ecosystems to extreme climate events: a systematic review and perspectives, Renew. Sustain. Energy Rev. 173 (Mar. 2023) 113038, https://doi.org/10.1016/j.rser.2022.113038.
[45] S. Suran, V. Pattanaik, and D. Draheim, "Frameworks for Collective Intelligence: A Systematic Literature Review," *ACM Comput. Surv.*, vol. 53, no. 1, p. 14:1-14:36, Feb. 2020, doi: 10.1145/3368986.
[46] D. Wolpert and K. Tumer, "An Introduction to Collective Intelligence," Sep. 1999.
[47] M.C. Schut, On model design for simulation of collective intelligence, Inf. Sci. 180 (1) (2010) 132–155, https://doi.org/10.1016/j.ins.2009.08.006.
[48] X. Qin, X. Li, Y. Liu, R. Zhou, J. Xie, Multi-agent cooperative target search based on reinforcement learning, J. Phys. Conf. Ser. 1549 (2) (Jun. 2020), https://doi.org/10.1088/1742-6596/1549/2/022104.
[49] M. Hosseini, A. Moazami, and V. M. Nik, "Collective Intelligence Function in Extreme Weather Conditions: High-Resolution Impact Assessment of Energy Flexibility on Building Energy Performance," in *Proceedings of the 5th International Conference on Building Energy and Environment*, L. L. Wang, H. Ge, Z. J. Zhai, D. Qi, M. Ouf, C. Sun, and D. Wang, Eds., in Environmental Science and Engineering. Singapore: Springer Nature, 2023, pp. 1395–1404. doi: 10.1007/978-981-19-9822-5_144.
[50] P.M. Krafft, E. Shmueli, T.L. Griffiths, J.B. Tenenbaum, A. "Sandy" Pentland, Bayesian collective learning emerges from heuristic social learning, Cognition 212 (Jul. 2021) 104469, https://doi.org/10.1016/j.cognition.2020.104469.
[51] M. Arulprakash, R. Jebakumar, People-centric collective intelligence: decentralized and enhanced privacy mobile crowd sensing based on blockchain, J. Supercomput. 77 (11) (Nov. 2021) 12582–12608, https://doi.org/10.1007/s11227-021-03756-x.
[52] D. Weinberg, Q. Wang, T.O. Timoudas, C. Fischione, A review of reinforcement learning for controlling building energy systems from a computer science

perspective, Sustain. Cities Soc. 89 (Feb. 2023) 104351, https://doi.org/10.1016/j.scs.2022.104351.
[53] A.T.D. Perera, P. Kamalaruban, Applications of reinforcement learning in energy systems, Renew. Sustain. Energy Rev. 137 (Mar. 2021) 110618, https://doi.org/10.1016/j.rser.2020.110618.
[54] A. Krishna G.S., T. Zhang, O. Ardakanian, M.E. Taylor, Mitigating an adoption barrier of reinforcement learning-based control strategies in buildings, Energy Build. 285 (2023), https://doi.org/10.1016/j.enbuild.2023.112878.
[55] D. Qiu, J. Xue, T. Zhang, J. Wang, M. Sun, Federated reinforcement learning for smart building joint peer-to-peer energy and carbon allowance trading, Appl. Energy 333 (2023), https://doi.org/10.1016/j.apenergy.2022.120526.
[56] R. Shen, et al., Advanced control framework of regenerative electric heating with renewable energy based on multi-agent cooperation, Energy Build. 281 (2023), https://doi.org/10.1016/j.enbuild.2023.112779.
[57] M. Khan, B.N. Silva, O. Khattab, B. Alothman, C. Joumaa, A transfer reinforcement learning framework for smart home energy management systems, IEEE Sens. J. 23 (4) (2023) 4060–4068, https://doi.org/10.1109/JSEN.2022.3218840.
[58] H. Syed Asad, H. Wan, H. Kasun, S. Rehan, G. Huang, Distributed real-time optimal control of central air-conditioning systems, Energy Build. 256 (2022), https://doi.org/10.1016/j.enbuild.2021.111756.
[59] B. Zhang, W. Hu, X. Xu, T. Li, Z. Zhang, Z. Chen, Physical-model-free intelligent energy management for a grid-connected hybrid wind-microturbine-PV-EV energy system via deep reinforcement learning approach, Renew. Energy 200 (2022) 433–448.
[60] V.M. Nik, M. Hosseini, CIRLEM: a synergic integration of collective intelligence and reinforcement learning in energy management for enhanced climate resilience and lightweight computation, Appl. Energy 350 (Nov. 2023) 121785, https://doi.org/10.1016/j.apenergy.2023.121785.
[61] P. Lund, J. Lindgren, J. Mikkola, and J. Salpakari, "Review of energy system flexibility measures to enable high levels of variable renewable electricity," 2015, doi: 10.1016/J.RSER.2015.01.057.
[62] G. Strbac, Demand side management: benefits and challenges, Energy Policy 36 (12) (Dec. 2008) 4419–4426, https://doi.org/10.1016/j.enpol.2008.09.030.
[63] A.M. Carreiro, H.M. Jorge, C.H. Antunes, Energy management systems aggregators: a literature survey, Renew. Sustain. Energy Rev. 73 (Jun. 2017) 1160–1172, https://doi.org/10.1016/j.rser.2017.01.179.
[64] C. McIlvennie, A. Sanguinetti, M. Pritoni, Of impacts, agents, and functions: an interdisciplinary meta-review of smart home energy management systems research, Energy Res. Soc. Sci. 68 (Oct. 2020) 101555, https://doi.org/10.1016/j.erss.2020.101555.
[65] L. Gelazanskas, K.A.A. Gamage, Demand side management in smart grid: a review and proposals for future direction, Sustain. Cities Soc. 11 (Feb. 2014) 22–30, https://doi.org/10.1016/j.scs.2013.11.001.
[66] J.R. Vázquez-Canteli, Z. Nagy, Reinforcement learning for demand response: a review of algorithms and modeling techniques, Appl. Energy 235 (Feb. 2019) 1072–1089, https://doi.org/10.1016/j.apenergy.2018.11.002.
[67] A.T.D. Perera, P.U. Wickramasinghe, V.M. Nik, J.-L. Scartezzini, Machine learning methods to assist energy system optimization, Appl. Energy 243 (Jun. 2019) 191–205, https://doi.org/10.1016/j.apenergy.2019.03.202.
[68] M. Thomas and A. Syse, "A historic shift: More elderly than children and teenagers," ssb.no. Accessed: Dec. 18, 2021. [Online]. Available: https://www.ssb.no/en/befolkning/artikler-og-publikasjoner/a-historic-shift-more-elderly-than-children-and-teenagers.
[69] Z.S. Venter, H. Figari, O. Krange, V. Gundersen, Environmental justice in a very green city: spatial inequality in exposure to urban nature, air pollution and heat in Oslo, Norway, Sci. Total Environ. 858 (Feb. 2023) 160193, https://doi.org/10.1016/j.scitotenv.2022.160193.
[70] Science Norway, "Climate expert: Norwegians do not understand how dangerous these heat waves are." Accessed: Jun. 16, 2023. [Online]. Available: https://sciencenorway.no/climate-change-global-warming-heat-waves/climate-expert-norwegians-do-not-understand-how-dangerous-these-heat-waves-are/2055011.
[71] S. Hosseini, P. Hajialigol, M. Aghaei, S. Erba, V. Nik, and A. Moazami, "Improving Climate Resilience and Thermal Comfort in a Complex Building through Enhanced Flexibility of the Energy System," in *2022 International Conference on Smart Energy Systems and Technologies (SEST)*, Sep. 2022, pp. 1–6. doi: 10.1109/SEST53650.2022.9898453.
[72] M. Asif, Chapter 3 - sustainable energy transition in the 21st century, in: M. Asif (Ed.), Handbook of Energy and Environmental Security, Academic Press, 2022, pp. 27–38, https://doi.org/10.1016/B978-0-12-824084-7.00023-0.
[73] A.M. Adil, Y. Ko, Socio-technical evolution of decentralized energy systems: a critical review and implications for urban planning and policy, Renew. Sustain. Energy Rev. 57 (May 2016) 1025–1037, https://doi.org/10.1016/j.rser.2015.12.079.
[74] A.T.D. Perera, V.M. Nik, D. Mauree, J.-L. Scartezzini, Electrical hubs: an effective way to integrate non-dispatchable renewable energy sources with minimum impact to the grid, Appl. Energy 190 (Mar. 2017) 232–248, https://doi.org/10.1016/j.apenergy.2016.12.127.
[75] M. Kottek, J. Grieser, C. Beck, B. Rudolf, F. Rubel, World map of the köppen-Geiger climate classification updated, Meteorol. z. 15 (May 2006) 259–263, https://doi.org/10.1127/0941-2948/2006/0130.
[76] M. Hosseini, K. Javanroodi, V.M. Nik, High-resolution impact assessment of climate change on building energy performance considering extreme weather events and microclimate – investigating variations in indoor thermal comfort and degree-days, Sustain. Cities Soc. 78 (2022), https://doi.org/10.1016/j.scs.2021.103634.
[77] A. Gasparrini, et al., Mortality risk attributable to high and low ambient temperature: a multicountry observational study, The Lancet 386 (9991) (Jul. 2015) 369–375, https://doi.org/10.1016/S0140-6736(14)62114-0.
[78] V.M. Nik, Making energy simulation easier for future climate - synthesizing typical and extreme weather data sets out of regional climate models (RCMs), Appl. Energy 177 (2016) 204–226, https://doi.org/10.1016/j.apenergy.2016.05.107.
[79] V. M. Nik, *Climate Simulation of an Attic Using Future Weather Data Sets-Statistical Methods for Data Processing and Analysis*. Chalmers Tekniska Hogskola (Sweden), 2010. Accessed: Feb. 03, 2024. [Online]. Available: https://search.proquest.com/openview/ea912d12f5d51c3928e7c855128251e9/1?pq-origsite=gscholar&cbl=18750&diss=y.
[80] "EnergyPlus." Accessed: Feb. 06, 2023. [Online]. Available: https://energyplus.net/.
[81] "Ladybug Tools | Home Page." Accessed: Feb. 06, 2023. [Online]. Available: https://www.ladybug.tools/.
[82] S. Corp, "Glossary | IFC." Accessed: Feb. 06, 2023. [Online]. Available: https://www.spatial.com/resources/glossary/what-is-ifc.
[83] ASHRAE, "ASHRAE Guideline 14-2014 Measurement of Energy, Demand and Water Savings." American Society of Heating, Ventilating, and Air Conditioning Engineers, Atlanta, Georgia, 2014. [Online]. Available: www.ashrae.org.
[84] G.R. Ruiz, C.F. Bandera, Validation of calibrated energy models: common errors, Energies 10 (10) (Oct. 2017) 1587, https://doi.org/10.3390/en10101587.
[85] D. Rutten, Galapagos: on the logic and limitations of generic solvers, Archit. Des. 83 (Mar. 2013), https://doi.org/10.1002/ad.1568.
[86] L. Pagliano, S. Carlucci, F. Causone, A. Moazami, G. Cattarin, Energy retrofit for a climate resilient child care Centre, Energy Build. 127 (Sep. 2016) 1117–1132, https://doi.org/10.1016/j.enbuild.2016.05.092.
[87] "Home - System Advisor Model - SAM." Accessed: Jan. 31, 2023. [Online]. Available: https://sam.nrel.gov/.
[88] "About NREL." Accessed: Jan. 31, 2023. [Online]. Available: https://www.nrel.gov/about/index.html.
[89] H. Abdullah, A. Gastli, and L. Ben-Brahim, "Reinforcement Learning Based EV Charging Management Systems–A Review," *IEEE Access*, vol. PP, pp. 41506–41531, Feb. 2021, doi: 10.1109/ACCESS.2021.3064354.
[90] L. Igualada, C. Corchero, M. Cruz-Zambrano, F.-J. Heredia, Optimal energy Management for a Residential Microgrid Including a vehicle-to-grid system, IEEE Trans. Smart Grid 5 (4) (2014) 2163–2172, https://doi.org/10.1109/TSG.2014.2318836.
[91] K. Liu, X. Hu, Z. Yang, Y. Xie, S. Feng, Lithium-ion battery charging management considering economic costs of electrical energy loss and battery degradation, Energy Convers. Manag. 195 (2019) 167–179.
[92] J. Van Roy, N. Leemput, F. Geth, J. Büscher, R. Salenbien, J. Driesen, Electric vehicle charging in an office building microgrid with distributed energy resources, IEEE Trans. Sustain. Energy 5 (4) (2014) 1389–1396.
[93] T. Sasaki and D. Biro, "Cumulative culture can emerge from collective intelligence in animal groups," *Nat. Commun.*, vol. 8, no. 1, Art. no. 1, Apr. 2017, doi: 10.1038/ncomms15049.
[94] K. Tumer, D. Wolpert, Collective Intelligence and Braess' Paradox. (2000) 109.
[95] A. Zhou *et al.*, "Watch, Try, Learn: Meta-Learning from Demonstrations and Reward." arXiv, Jan. 30, 2020. doi: 10.48550/arXiv.1906.03352.
[96] L. Clemmensen, "Sparse Discriminant Analysis," *Technometrics*, Jan. 2011, Accessed: Jan. 30, 2023. [Online]. Available: https://www.academia.edu/44190644/Sparse_Discriminant_Analysis.
[97] H. Haji Ali Afzali and J. Karnon, "Specification and Implementation of Decision Analytic Model Structures for Economic Evaluation of Health Care Technologies," in Encyclopedia of Health Economics, A. J. Culyer, Ed., San Diego: Elsevier, 2014, pp. 340–347. doi: 10.1016/B978-0-12-375678-7.01401-2.
[98] C.J.C.H. Watkins, P. Dayan, Q-learning, Mach. Learn. 8 (3) (May 1992) 279–292, https://doi.org/10.1007/BF00992698.
[99] R. Sutton and A. Barto, *Reinforcemnet Learning, An introduction*, Second. Cambridge, Massachusetts: The MIT Press. [Online]. Available: https://lccn.loc.gov/2018023826.
[100] E. Levin, R. Pieraccini, and W. Eckert, "Using Markov decision process for learning dialogue strategies," in *Proceedings of the 1998 IEEE International Conference on Acoustics, Speech and Signal Processing, ICASSP '98 (Cat. No.98CH36181)*, May 1998, pp. 201–204 vol.1. doi: 10.1109/ICASSP.1998.674402.
[101] J. Clifton, E. Laber, Q-learning: theory and applications, Annu. Rev. Stat. Its Appl. 7 (1) (2020) 279–301, https://doi.org/10.1146/annurev-statistics-031219-041220.
[102] N. Bäuerle and U. Rieder, "Theory of Finite Horizon Markov Decision Processes," 2011, pp. 13–57. doi: 10.1007/978-3-642-18324-9_2.
[103] EN 16798-1:2019-Indoor environmental input parameters for design and assessment of energy performance of buildings add. 2019.
[104] CIBSE, "Guide A, environmental design (7th ed.)." Chartered Institution of Building Services Engineers, London, UK, 2006.
[105] *ANSI/ASHRAE Standard 55-2020. Thermal Environmental Conditions for Human Occupancy*. 2020, p. 80. [Online]. Available: https://www.ashrae.org/technical-resources/bookstore/standard-55-thermal-environmental-conditions-for-human-occupancy.
[106] International Standard Organization, *ISO 7730:2005. Ergonomics of the thermal environment – Analytical determination and interpretation of thermal comfort using calculation of the PMV and PPD indices and local thermal comfort criteria.* 2005.
[107] World Health Organisation, "Health Impact of Low Indoor Temperatures." 1987.

[108] "TM 52 Limits of thermal comfort: avoiding overheating in European buildings, Chartered Institution of Building Services Engineers - Publication Index | NBS." 2013. Accessed: Jun. 17, 2023. [Online]. Available: https://www.thenbs.com/PublicationIndex/documents/details?Pub=CIBSE&DocID=304234.

[109] R. Luthander, J. Widén, D. Nilsson, J. Palm, Photovoltaic self-consumption in buildings: a review, Appl. Energy 142 (Mar. 2015) 80–94, https://doi.org/10.1016/j.apenergy.2014.12.028.

[110] "16798-2:2019 - Energy performance of buildings - Ventilation for buildings - Part 2: Interpretation of the requirements in EN 16798-1 - Indoor environmental input parameters for design and assessment of energy performance of buildings addressing indoor air quality, thermal environment, lighting and acoustics (Module M1-6)." EUROPEAN COMMITTEE FOR STANDARDIZATION.